

SOLITON FORCE MICROSCOPY USING CAVITY SOLITON

A thesis submitted in partial fulfillment of the requirements for the award of
degree of

Master of Science

In

Physics

Submitted by:

HARLEEN KAUR

Roll No. 301504015

Under the guidance of

DR. SOUMENDU JANA

Associate Professor

SPMS,

Thapar University, Patiala



School of Physics and Materials Science

Thapar University,

Patiala-147001, INDIA

July 2017

*For their love, support and encouragement
I dedicate this work to my parents and to the most
adorable person of my life my brother “Mandeep”*

CERTIFICATE

I hereby declare that the work which has been presented in this thesis entitled "Soliton force microscopy using cavity soliton" is an authentic record of my own work carried out for the partial fulfillment of the requirement for the award of the degree of Masters of Science in Physics at Thapar University, Patiala (Punjab), under the guidance of **Dr. Soumendu Jana**, Associate Professor, School of Physics and Materials Science and refers other researcher's work which are duly listed in the reference section. The intellectual content of this thesis is the product of my own work and contains no material which to a substantial extent has been accepted for the award of any other degree at this or any other educational institution, except where due acknowledgment is made in the thesis.

Harleen Kaur

Harleen Kaur

Date : 17/7/2017

Roll No.:301504015

It is to certify that the above statement made by the candidate is correct and true to the best of my knowledge and belief.

Soumendu Jana
Dr. Soumendu Jana

Associate Professor

**School of Physics and Material Science
Thapar University, Patiala**

ACKNOWLEDGEMENT

Work on this thesis would not have been possible without the encouragement and the support of many people. I would like to express my sincere gratitude especially to the following:

The first and greatest thank to my supervisor **Dr. Soumendu Jana** for his continuous support and supervision, for his excellent guidance, patience, motivation and enthusiasm. I could not have imagined having a better advisor and mentor than him for my thesis.

I would like to thank **Dr. Manoj Kumar Sharma** for providing me with an excellent atmosphere and all the necessary facilities for my research. Besides, my supervisor, I would like to thank from the bottom of my heart, **Ms. Baldeep Kaur** and **Mr. Gurkirpal Singh**, Research Scholar, for sharing their valuable experiences and timely guidance. I would not have been able to complete my dissertation without their cooperation. I would like to thank my best friend **Yashjeet Kaur** for being their always with me.

Last but not the least, I would like to thank my parents and my elder brother for their unconditional support, both financially and emotionally throughout my degree.

Above all I render my gratitude to the almighty who bestowed upon me the strength and vision to walk on the path of truth.

Date:

Harleen Kaur

CONTENTS

CHAPTER-1 INTRODUCTION

1.1 Introduction	1
1.2 Literature Review	4
1.3 Motivation	7
1.4 Objective	7

CHAPTER-2 BASICS OF CAVITY SOLITON AND METHODOLOGY

2.1 Nonlinear Optics	8
2.2 Optical Soliton	9
2.3 Dissipative Soliton	11
2.4 Cavity Soliton	13
2.5 Vertical Cavity Surface Emitting Lasers (VCSEL)	15
2.6 Different microscopy	17
2.7 Methodology	19
2.7.1 Split Step Fourier Methods	20
2.7.2 Flow chart of Split Step Fourier Method	23

CHAPTER-3 RESULTS AND DISCUSSION

3.1 Mathematical Modeling	24
3.2 CS generation and dynamics with variation of pump power (μ) for active material	25
3.3 Formation and dynamics of CS with variation of 'γ' pump parameter for passive material	30
3.4 CS generation and dynamics with variation of μ pump parameter for active material	36

3.5 Formation and dynamics of CS with variation of γ pump parameter for passive material	40
3.6 CS dynamics with random gradient of parameter	44
Conclusion	46
List of figures	
References	

ABSTRACT

The movement of cavity soliton (CS) can be regulated by gradients of the system parameter. We studied the generation and dynamics of CS in VCSEL with saturable absorber (SA) and coupled with Frequency Selective Feedback (FSF) for different gradient and fluctuation of the system parameters. Periodic modulation, constant gradient and random fluctuation/gradient have been considered. Gradient modulation driven soliton dynamics for all these cases are presented extensively. The CS dynamics are found sensitive to the gradient. The result suggest that such CS dynamics can be used to scan a material surface as well as bulk any inhomogenities or defects of material can be detected intensively. This make the path for soliton force microscopy.

CHAPTER - 1

INTRODUCTION

1.1 Introduction:

Human eye has a limitation of viewing the things around us. Things of normal size can be viewed easily by human eye, without any external aid. But some abnormally small things can be viewed only with the help of microscopes. The field of using microscopes to view objects is termed as microscopy. Viewing objects by way of simple glass lenses is called optical microscopy while using electronic beam constitutes electron microscopy. But here we are going to introduce a new type of microscopy called 'soliton force microscopy'. This proposed a new type of microscopy which is not explored extensively. Soliton force microscopy is very sensitive tool for non-homogeneities in the media and also potentially increasing outside the soliton community (1). At the core of soliton force microscopy there is SOLITON, which is a localized self similar structure. Soliton can propagate long distances without visible changes (2). Due to vast applications such self-localized structures are interesting in optics (3). Soliton inside a dissipative cavity attracted huge attention. They can be used as future 'bit' for information.

Cavity soliton are localized structures which are bistable, self-sustained and independent local peaks of intensity over a uniform background which by a proper local optical disturbance can be switched on or off individually. Due to their common independence and plasticity, they are promising candidates and have attracted growing interest for data processing. Their control purpose at supplying all optical functionalities for information technology when observed in semiconductor microcavities. In absence of any statement about their exact nature confined structures can be used to reveal even extremely shallow non-homogeneities in the most of the nonlinear medium. In order to discover non-homogeneities the natural mode of localized structures is required. Each solution will have a zero eigenvalue related to the translational degrees of freedom if a system is unaffected by translation. Cavity soliton are stable and hence all their other eigenvalues have negative real part and any

disturbance will mostly paired to neutral mode, including translation. The movement of cavity soliton can be observed under the effects of externally applied gradients (4). The position of cavity soliton can be held by the gradient and it's possible to place the cavity soliton (a type of soliton) at the maximum intensity or phase gradient. A stationary position of cavity soliton in the presence of gradients of different origins will be those where the forces applied on them counterbalance. The dynamics of cavity soliton was observed under the effect of externally applied gradients. When the movement of cavity solitons is superimposed across the entire section of the system, non-homogeneities of the device is given by the frequency of the area. By creating a gradient the motion of cavity soliton is induced in the transversal direction to the generation of light (5).

Deviation of the trajectory of a cavity soliton set by the controlled gradients reveal the underlying inhomogeneities. Stable position of cavity soliton depends on spacial gradients in the system. Many inhomogeneities can grow in semiconductor systems during the postprocessing stages. Leading to a detailed study of surfaces even if several microscopy process can be applied to each separate component of a semiconductor system. Very few methods actually allow to examine the most of a fully grown structure besides basic spatially determined photoluminescence intensity, which is not very efficitive at revealing certain non-homogeneities (4). The quality of optics which bounds the uniformity of holding beam and preparation of the external gradients are the practical limitations. Soliton force microscopy is the process that not only permit to detect surface defects but can also examine bulk defects in the device. To reveal the defects, various potential felt by cavity solitons are used in the vertical cavity surface emitting laser (VCSEL). (5). For the formation and dynamics of cavity soliton, VCSEL is preferable due to its various advantages. Because of large cross-sectional area of VCSEL devices, gradient induced cavity soliton dynamics are detectable(6). To control the cavity soliton the inhomogeneities such as system parameter variation can be used. Particularly cavity soliton is required for soliton force microscopy. Lets briefly discuss about the concept of the soliton and its types.

Soliton became one of the most elating areas of research (7). In 1834, a Scottish engineer, John Scott Russell was first one to observe 'soliton' in a water canal and soliton was first named as the "wave of translation". But later in 1965, wave of

translation was recognized as 'soliton' by Martin Kruskal and Norman Zabusky. Solitons are localized or confined structures, wave packets which are capable of travelling with self-similar shape (8). They show properties related with the particle and interact with each other, hence named as 'soliton' (9). Solitons can be found in light waves, water waves, plasma and in many other medium (8). Optical solitons are most significant applications of nonlinear optics (10). Solitons fall into two broad categories:- conservative or dissipative soliton (DS). 'Conservative soliton' appear as a result of a counter-balance between diffraction and nonlinearity (11).

Due to their importance in a wide variety of fields DS have attracted great interest. DS are self-confined structures in non-equilibrium systems (3). They exist in systems having dissipations i.e. some gain or loss of energy and/or mass (12). The balance of linear and nonlinear effects shape a dissipative soliton, however the loss of energy of the system must be balanced by the energy input to the system (11). Spatial optical dissipative solitons are stable, self trapped beams of light, sitting on a uniform, or quasi-uniform, background. They have been recognized in photonic devices like semiconductor microcavities (10). The properties like pulsating dynamics and an internal energy exchange mechanism makes dissipative soliton appealing object for research (7). Due to their prospective applications in all-optical switching, pattern recognition and parallel information processing in recent years, both conservative and dissipative settings have attracted a great deal of interest (13).

The special class of dissipative soliton is cavity soliton(CS). CS are self-localized, self-confined pulses of light. The study of optical solitons in the late 1980's in dissipative cavities extended from the conditions of temporal effects generated by dispersion to spatial effects generated by diffraction. These spatial solitons utilized in all optical processing units are generally known as 'cavity solitons' (14). CS come out in the transverse plane of cavity as a bright(dark) intensity peaks over a dark(bright) homogenous background (15). They are independent from the system's boundaries and from each other and are bistable which means that they can be turned on and off by the means of coherent pulses (16). They belong to family of dissipative structures obtained far from equilibrium (17). Cavity soliton can develop interesting phenomena in photonic systems which are useful for applications in optical information processing. Cavity soliton share numerous properties of spatial solitons. In the cavity,

diffraction is balanced with nonlinear effects. Cavity soliton has freedom to move in localized direction (11). Even in the absence of holding beam, a device which is able to generate cavity solitons is called a Cavity Soliton Laser (CSL) (18). Applications of cavity soliton in all optical information storage and information technology are of high interest and are diverse in the field of photonics. Cavity soliton is used for all optical information processing, all delay lines, all optical logic gates and soliton force microscopy (15).

1.2 Literature Review:

The concept of dissipative soliton, since the last few decades was known properly. In 1965, introduced by Zabusky and Kruskal, the term ‘soliton’ was mentioned as localized solutions of integrable nonlinear systems. Such solutions preserve their shape and velocity after colliding with each other. In the beginning of 1990’s, a dramatic turning point occurred. It was discovered that soliton waves survive in a wide range of non-integrable and non-conservative system. For nomenclature purposes, new terminology was required to be innovated. Thus, soliton in nonlinear systems with nonlinear gain or loss mechanisms were called as ‘dissipative solitons’. For describing reaction-diffusion systems in the domain of plasma physics, the term ‘autosoliton’ was formulated. In a nonlinear medium, dissipative optical solitons are confined wavepackets of light and their stability as well as existence depend on the energy counter-balance(19).

Dissipative soliton is a localized structure in a nonlinear system and occur in a system far from equilibrium. Stable localized solitons exist because there is balance between non-linearity and dispersion or diffraction. Cell, organ and animal – objects at each biological level can be viewed as dissipative soliton(12). In the context of active-mode locking the abstract idea of dissipative soliton can be applied. Their use is remarkable in the field of passively mode-locked lasers to a greater extent that some systems are now termed as dissipative soliton laser (DSL). For understanding complex pulse dynamics, the concept of dissipative soliton offer an excellent framework. To test the concept of dissipative soliton the area of mode-locked lasers serves as an ideal playground. In nonlinear optics, experimental demonstration of

light bullets is one of the major challenges and light bullet could be effective for applications such as parallel optical data processing. For the experimental implementations of stationary light bullets the use of dissipative nonlinearities over a great range is considered to be the most promising strategy (19).

In the driven nonlinear optical cavities, dissipative soliton have been referred to as 'cavity soliton'. Cavity soliton have drawn a growing interest due to their importance in a wide variety of fields. In the recent years, the control, achievements and understandings of cavity solitons have shown remarkable progress (20). Cavity soliton are bright intensity peaks across a dark uniform background. Cavity soliton is bistable which means they can be present or absent under the same condition. (16). Some laser schemes have been presented to maintain cavity solitons. For a major laser technology, lasing cavity soliton has been generated(20). A device generating cavity soliton without holding beam is called cavity soliton laser and has a enormous advantages in terms of simplicity, robustness, compactness or denseness (21). CSL convert broad-area excitations into a narrow, coherent, high quality power pulse. Lasing cavity soliton is free to choose phase, frequency and polarization. Because of fast response, compactness and ease of integration semiconductor microcavities are essential for photonic applications (20).

A transition from a stable to oscillating localized structure in 1-D were experimentally determined and analytically explained for liquid crystal light valve system in the absence of delayed feedback. On the dynamics of spatially extended systems the effect of the delayed feedback is a current area of research. A framework for the study of cavity soliton was proposed recently in broad area VCSEL (vertical cavity surface emitting lasers). The effect of the delayed feedback was theoretically studied on the properties of 2-D cavity soliton (22).

By introducing phase or amplitude gradients in the holding beam cavity soliton can be utilized as mobile pixels for all optical processing units. Because of growing use of cavity soliton in semiconductor have attracted a growing interest. They unite the bistability and plasticity properties with the advantages of semiconductor media in terms of speed and small size (21). Because of phase-amplitude coupling, bistability was observed because of which the different carrier densities of the lasing and non-

lasing states imply different refractive indices (20). In order to create bistability, saturable absorber is added to the lasing cavity (23).

Rosanov and co-workers determined a theoretical prediction of dissipative soliton in a laser with a saturable absorber (16). With saturable absorbers the most interesting results have been obtained. In these optical systems according to numerical and analytical results it is possible to monitor localized structures. Each localized structure behave as an independent object because correlation length of a confined structure is much smaller than the size of the system (5). Involving several cavity modes, the soliton generated in the laser can be either stationary in intensity (single frequency) or oscillating intensity (multiple frequency). For a practical transversal soliton laser, frequency selective feedback have attracted great area of interest (23).

Owing to potential applications to information technology, in nonlinear system immense work was undertaken in the area of spatial pattern formation. Due to strong correlation between several parts of an optical pattern, local modification which was introduced to encode information also affected the other parts. This problem can be solved by producing cavity soliton. By introducing in the driving field a spatial modulation, the place of cavity soliton can be fixed. By introducing an appropriate phase shift in the address pulse, the position of cavity soliton can be erased. The capability of writing and erasing cavity soliton by laser pulses was confirmed experimentally in organic saturable absorbers. For information encoding the most attractive system recently observed are the semiconductor devices which by using 2-D spatial soliton are reported both theoretically and experimentally in model systems. Stable solitons both in below-threshold vertical-cavity lasers can be recognized and controlled (24).

The solitons can spontaneously move in a cavity soliton laser based on a VCSEL with a saturable absorber (18). Broad-area VCSEL with saturable absorber has been studied theoretically and the presence of cavity soliton was noticed numerically in the system (16). To apply cavity soliton in semiconductor material system the broad-area VCSEL appear as an ideal device (5). Cavity soliton is utilized for all optical information processing and for VCSEL's characterization.

Some properties of the system in non-uniform medium are different in different directions. Non-homogeneity of the medium has a important role on cavity soliton. Experimentally and numerically local non-homogeneties have the pinning role in the stable position of confined structures. Neutral mode of localized structures was build in order to detect inhomogeneities. Many inhomogeneties in semiconductor system can arise during the post-processing or growing stages. The position of cavity soliton is dependent on spatial gradients in the system parameters. In order to control the position of cavity soliton the inhomogeneities such as system parameter variation can be used (4).

1.3 Motivation:

Any gradient creates cavity soliton dynamics. This can be used to scan different surfaces and bulk for example tissues, membranes. Although very interesting, to the best of our knowledge proper attention is not paid to study gradient induced scanning using cavity soliton. Particularly cavity soliton can be used for soliton force microscopy. We propose to utilise the gradient driven cavity soliton in soliton force microscopy.

1.4 Objective:

The main objectives of our investigation are:-

- To study the dynamics of cavity soliton.
- To utilize the gradient driven cavity soliton in soliton force microscopy.

CHAPTER – 2

BASICS OF CAVITY SOLITON AND METHODOLOGY

To understand the CS and its working the basic knowledge of soliton and related nonlinear and linear phenomena are important. In this chapter we briefly discuss those basics, also our investigation is driven by numerical experiments. The numerical methodology has been elaborated in this chapter. We also describe the device that hold CS. We also talked about different microscopies.

2.1 Nonlinear optics:

The nature of interaction was believed to be linear between light and matter, before the invention of laser. The electric polarization (P) of the optical material in this case is proportional to the electric field (E) in a linear way of the incident radiation. Immediately after the first demonstration of laser in 1960 by Ted Maiman the nonlinear optics era was started. Nonlinear optics arise when a intense light interact with a matter. Nonlinear optics also referred as ‘optics of intense light’ phenomena to study the behavior of light in the medium of nonlinearity. Dielectric polarization (P) in nonlinear media responds nonlinearly to the electric field (E) of the light.

In 1961 the discovery of second harmonic generation by P.A. Franken is marked as starting point of nonlinear optics. A year later in 1962, the work of N. Bloembergen and his co-workers on optical wave mixing give a thrust to research on nonlinear optics. A field $\sim 1\text{kV/cm}$ is required in the optical medium to induce nonlinearity corresponding to a beam intensity of $\sim 2.5\text{ kW/cm}^2$. Such intense beam is provided by only laser sources. The nonlinearity is typically observed by laser light i.e. at very high intensities. The high intensities opened up the new field of optics. A vast number of nonlinear optical effects exist that not only possess potential applications but are also of fundamental interest. The total number of nonlinear optical effects is larger than linear optical phenomena. All simple and complex phenomena can be explained in nonlinear medium. The superposition principle is no longer valid in nonlinear optics (8).

Normal light is weak as compared to the highly intense light. In nonlinear optics study it does not work. By linear optics many phenomena can't be understood. For studying complex phenomena nonlinear optics provide a new approach and a better platform. Origin of soliton is related to nonlinear optics because it has a capability to generate soliton.

Because of its diverse applications in many areas from telecommunications to biomedical instrumentations, from homeland security to space applications the nonlinear optics has remained an active field of research and has continued to grow at fast pace. Nonlinear optics is used in optical communication, optical computing, optical switching and in frequency generation. Hence, nonlinear optics emerges as a topic having broadest scope providing endless path for research.

2.2 Optical Soliton:

'Solitons' are localized structures that preserve its shape and size even after it collides with other soliton. Soliton are found in light waves, water waves, plasma and in many other media. They are capable of propagating with self-similar shape. Nonlinearity of medium is required for the formation of soliton. In 1834, a Scottish engineer, John Scott Russell firstly observed soliton in a water waves of union canal and named it as 'wave of translation' (8). But later in 1965, wave of translation was recognized as soliton by Martin Kruskal and Norman Zabusky. Both of them found stable wave solutions by rederiving the KdV equation. These solutions maintain their shape and velocities even after interaction. They named such waves SOLITON. Soliton preserve their properties even after interacting with each other and then act like a particle. They are solitary waves and used to refer to confined solutions of integrable nonlinear systems. In modern mathematical physics, the concept of soliton become so developed that it is being assumed that any wave can give rise to a soliton (25).

Optical solitons are most essential applications of nonlinear optics and have been studied in various systems since its first observations in 1980 and also give rise to a large variety of solitons. Optical soliton is a self-confined state of pulse or beam in which nonlinearity balances dispersion. Depending on their state of being confined in

time or space domain, temporal soliton and spatial soliton are two categories of optical soliton. Temporal soliton also called longitudinal soliton are pulses that remained confined in time domain. Self - trapped localized pulse that are confined in transverse direction of propagation are called spatial solitons. When a beam of light remain self-localized in both time as well as space domain it is called spatiotemporal soliton or light bullets.

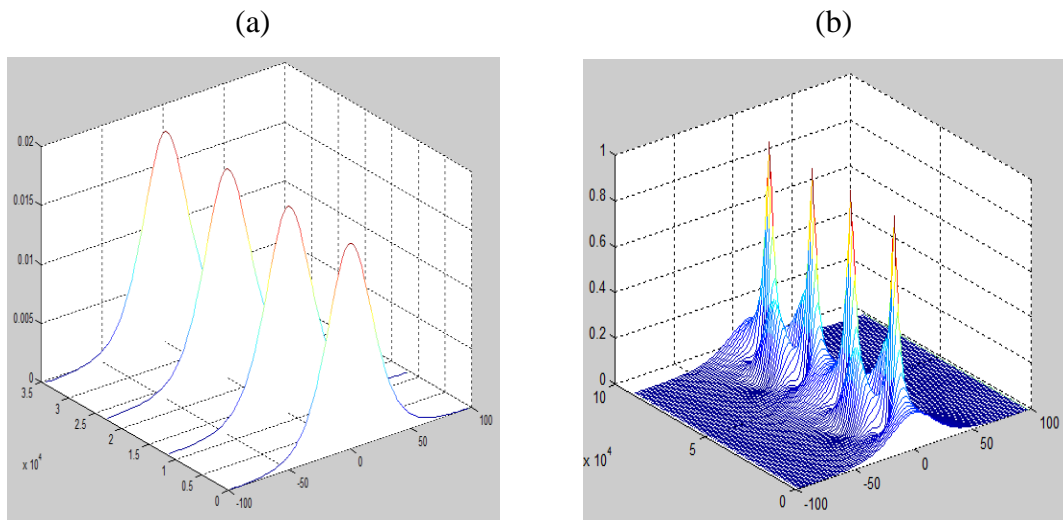


Figure 2.1 (a) Fundamental Soliton and (b) Second order soliton

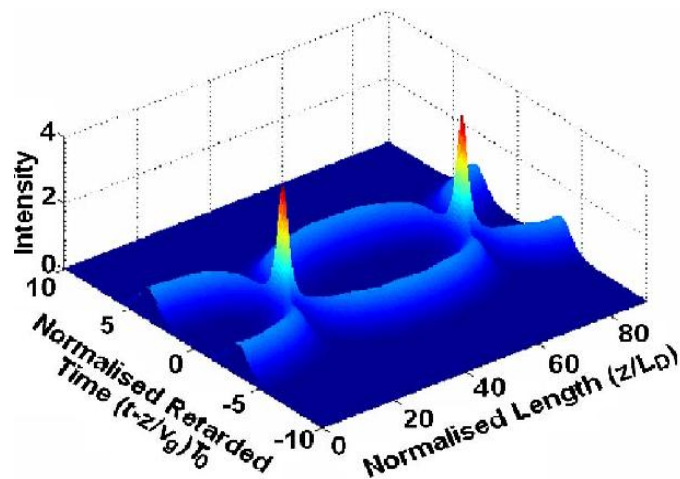


Figure 2.2 Soliton collision

Soliton can grow both in conservative and non-conservative system. ‘Conservative soliton’ come out as a result of counter-balance between diffraction and nonlinearity. In conservative soliton there is no loss of energy from the system and no energy input

to the system. While in ‘non-conservative’ system there is some gain or loss of energy. Hence, the soliton in non-conservative system are called dissipative soliton (11).

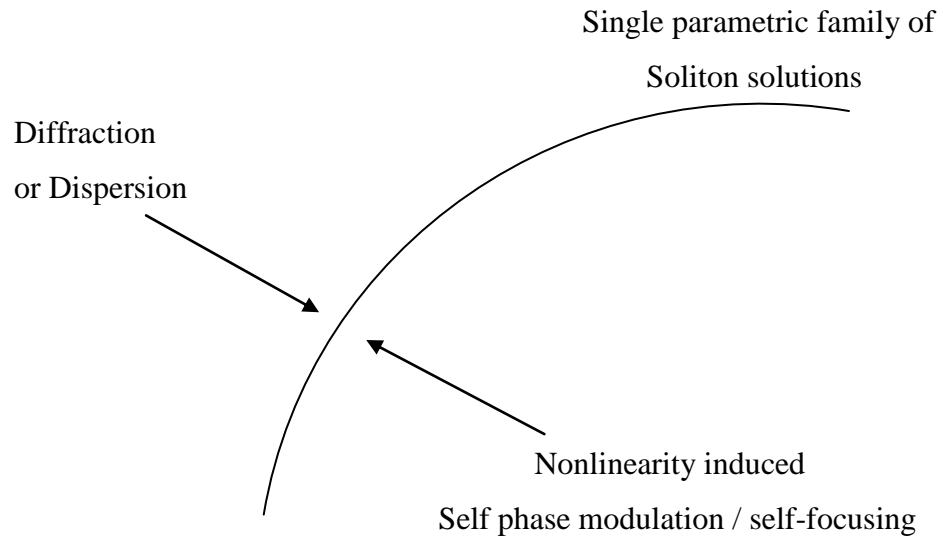


Figure 2.3 Conservative Soliton (2)

2.3 Dissipative soliton:

Even after colliding with each other, solitons maintain their velocity and shape. It was originally mentioned to be localized solutions of integrable nonlinear systems. But a dramatic turning point occurred when it was discovered that solitary waves existed in a broad range of non-integrable and non-conservative systems. Soliton waves in nonlinear optical systems with a nonlinear gain or loss mechanism are called ‘dissipative soliton’. The stability and existence of dissipative solitons depend on the energy balance (19). They emerge as a result of a balance between gain and loss as well as a balance between dispersion and nonlinearity. The existence of a dissipative soliton is observed as soon as some external energy is supplied to the system and disappears when the energy supply is discontinued and depends on processes like dispersion/diffraction, nonlinearity, gain, and loss.

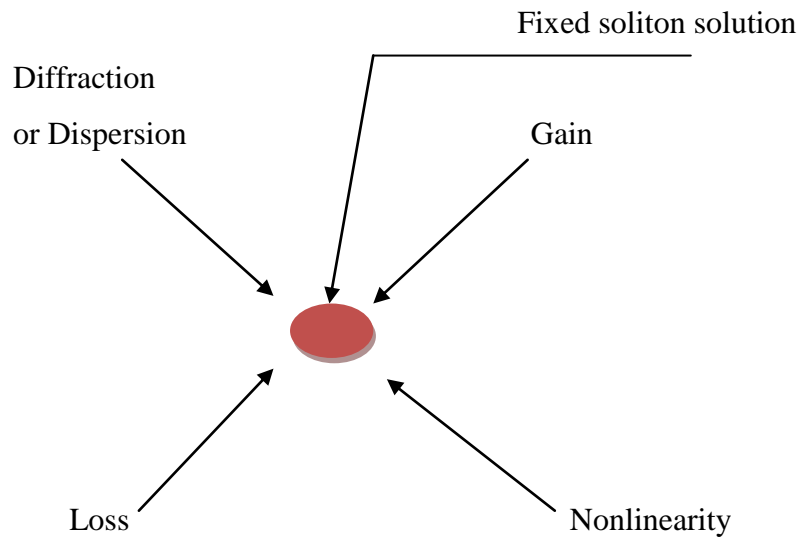


Fig 2.4 Dissipative Soliton (2)

Hence, conservative system is in which Diffraction + Nonlinearity are balanced.

Dissipative system is in which Diffraction + Nonlinearity and Gain + Loss are balanced.

Dissipative soliton is a localized structure. This structure could be profile of temperature, magnetic field, light intensity etc (12). Self confined dissipative structures are referred as ‘localized states’, ‘localized structures’ or spatial dissipative soliton in the nonlinear medium. Spatial dissipative soliton are stable, self-localized beams of light on a uniform or quasi uniform background. In photonic devices they have been recognized like semiconductor microcavities. It acts as a bit of information (10).

Due to their application in wide variety of fields dissipative soliton have been a promising candidate. Providing a new approach dissipative soliton become a fascinating area of research by manifesting conditions for self-organization (3). Stable soliton are supported by dissipative soliton. Their properties are different from those mentioned in the KdV equation. Their solutions, shape, velocity, amplitude all are constant and defined system’s parameters (7).

DS exists in a physical, chemical and biological system. To generate a dissipative soliton one of the most common way is by injecting an optical signal into laser cavity

which carry a nonlinear medium in combination with an intensity discrimination mechanism (14). Without splitting or distortion, dissipative soliton can hold large nonlinear phase shifts. With tremendously high energy and peak power they are stable (26). Because of their growing use and interest in the field of passively mode-locked lasers some systems are referred as dissipative soliton laser (DSL) (19). Dissipative soliton laser with much higher energies support stable pulses because of which they are promising candidate for photophysical applications such as multiphoton microscopy (27).

2.4 Cavity Soliton:

Localized structures with a single intensity peak is called ‘cavity soliton’ (5). Cavity soliton are localized pulse of light appearing as a bright (dark) intensity peak over a dark (bright) homogenous background (15). Cavity soliton are the special class of dissipative soliton in optical cavities found far from equilibrium (17). Cavity soliton are self-confined states existing in a cavity filled with a nonlinear medium (21). Cavity soliton behave as an independent objects because its correlation length is much smaller than system’s size (5). Cavity soliton are independent from the boundary of the system and are bistable which means that they can be absent or present by the means of coherent pulses (16). Cavity soliton have freedom to move in localized direction (1). Because of their growing use cavity soliton give rise to interesting phenomena which are useful for applications in optical information processing (11). In a laser, Rosanov and co-workers proposed the theoretical prediction of dissipative localized structures with a saturable absorber (16). Various systems in optics maintain cavity soliton, mainly VCSEL. The system includes holding beam, writing beam, nonlinear medium and mirrors. Nonlinear medium called as active gain/ loss medium which with optical and electrical pumping provide gain. To reflect the incoming beam, the nonlinear medium is closed by high reflecting mirrors. To compensate the loss a broad area beam called holding beam is added. Writing beam is the focused optical pulse derived from same laser as holding beam.

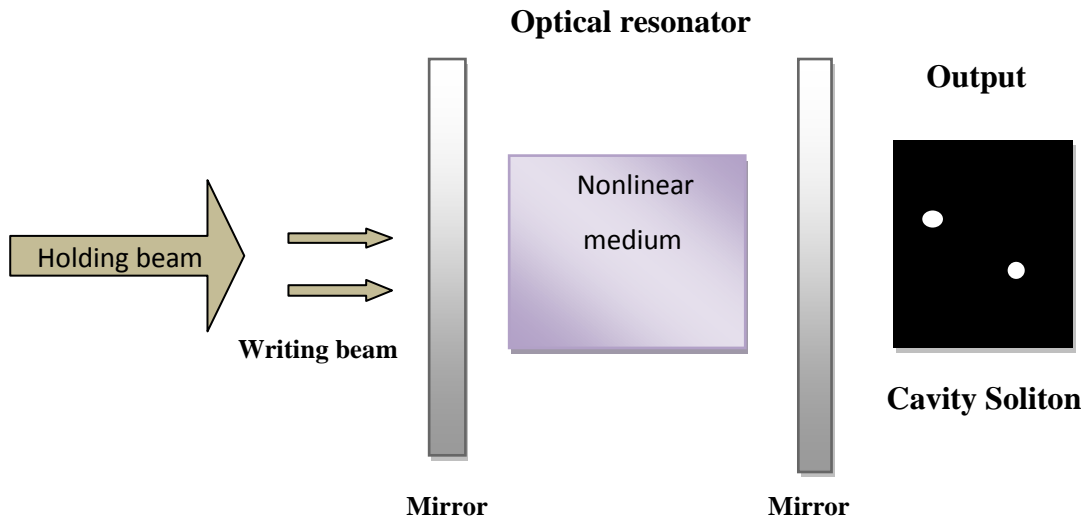


Figure 2.5 Optical cavity soliton

(image concept:- www.funFACS.com)

Cavity soliton laser described as self-confined microlaser is a device which is capable of generating cavity soliton without holding beam (18). In terms of simplicity, robustness and compactness cavity soliton laser has a vast or tremendous advantages (21). It has the freedom to select phase, frequency and polarization (20). The freedom of a lasing cavity soliton to choose its own frequency and phase is the main difference between a cavity soliton (CS) and cavity soliton laser (CSL). Cavity soliton occur in driven system where to inject energy into the system an external holding beam is required whereas in case of CSL to give energy holding beam is not required. The frequency and phase remain free because of no holding beam in these system (11). Recently three types of CSL have been observed. The first one is a VCSEL with a frequency selective feedback, followed by two coupled VCSEL in a face-to-face configuration and the third one is monolithic VCSEL with a saturable absorber. All of the three types have vertical cavity surface emitting laser (VCSEL) as the basic element (28).

Broad area VCSEL plays an significant role in the development of study of cavity soliton in semiconductor systems (5). Cavity soliton have attracted a growing interest in semiconductor. In terms of speed and small size they combine the bistability and plasticity properties with the advantages of semiconductor media (21). To implement cavity soliton in semiconductor material system the broad area VCSEL appear as an ideal device (5).

Providing a significant approach to microlasers, CSL convert a broad-area incoherent excitations into a narrow, coherent or high quality power beam (3). The experimental demonstration of a saturable absorber based semiconductor CSL with two mutually paired broad-area semiconductor resonators where one plays the role of laser (pumped above transparency) and other plays the role of the saturable absorber has been achieved recently (18).

Applications of cavity soliton in all optical information storage and information technology are of growing interest and are diverse in the field of photonics. Cavity soliton is used for all optical information processing, all delay lines, all optical logic gates, soliton force microscopy and for VCSEL's characterization.

2.5 Vertical Cavity Surface Emitting Laser (VCSEL)

The vertical cavity surface emitting lasers are a type of semiconductor laser whose structure is different from conventional stripe lasers. By the boundary of epitaxial layers the vertical cavity is formed and from the mirror surfaces the output light is taken. In 1979, the first device where a 1300nm wavelength GaAsP-InP material used for the active region came out (29).



Figure 2.6 Typical VCSEL

(Image concept:- Thorlabs)

Because of their growing use the importance of VCSEL is reflected in the fact that among all types of semiconductor lasers today they have the second largest production volume (30). For laser operation around 980nm the VCSEL is being designed and optimized for high power. Enclosed in an AlGaAs spacer to construct

the one-wavelength thick cavity, the active region is composed of three GaAs quantum wells. Two Bragg mirrors of high reflectivity sandwiched the active layer. The back mirror is n-doped with silicon while the front mirror is p-doped with carbon. Cavity resonance of 980nm, the back and front mirror have 30 and 24.5 pairs of quarter wavelength respectively. Using molecular beam epitaxy the whole cavity is originated on a GaAs substrate (5). For organization of cavity soliton and transverse localized structures, VCSEL's are capable of satisfying the necessary or required conditions (31). For establishment of cavity soliton optically pumped broad-area VCSEL is used. To implement cavity soliton in semiconductor material system, broad-area VCSEL seems as an ideal device. For high power lasers optically pumping is commonly used in VCSELs. For the demonstration of cavity soliton in semiconductor optical amplifier, the VCSEL design has been successfully designed. (5). On a single GaAs chip a large number of electrically pumped VCSEL of few μm are constructed (32).

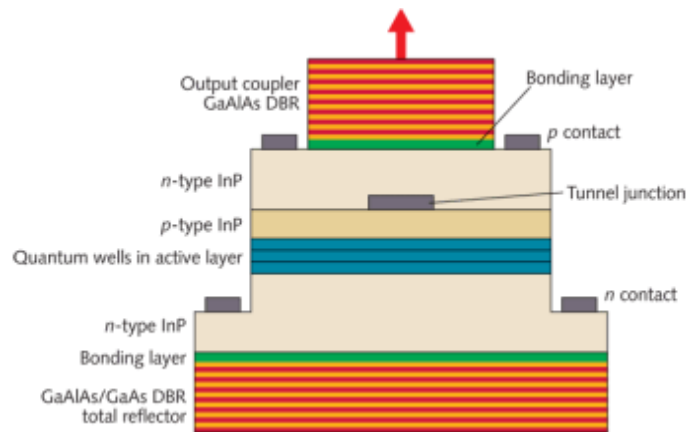


Figure 2.7 Structure of VCSEL

(Image courtesy:www.laserfocusworld.com)

VCSEL shows a variety of applications. It has low manufacturing cost and reliability, single mode operation, high temperature gradient and higher output power. For operation, the lowest threshold edge-emitting lasers require approximately 0.55mA. VCSEL has low threshold current (few μA) and longer operating lifetime (32). Electrically pumped and easy to regulate, semiconductor lasers which are also small and integrable have high efficiencies (31). VCSEL provide high intensity light than

simple diode laser or edge emitting. The difference between VCSEL and edge emitting is shown below:-

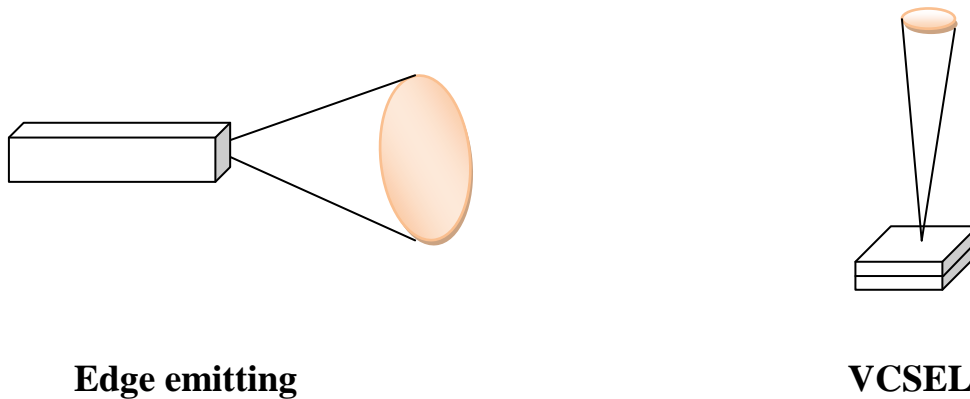


Figure 2.8 Edge emitting and VCSEL

Applications in all optical delay lines, VCSEL's fast time response makes them attractive. For optical control of light, optical information storage and processing, VCSEL have a potential and essential applications (33). Because of its various advantages VCSEL is preferred over edge emitter for generation and dynamics of cavity soliton (6).

2.6 Different Microscopy

Microscopy can be separated into several different classes. Optical microscopy uses light to image the sample and is first to be invented. A essential alternative to light microscopy was developed in the early 20th century where to generate the image electrons were used rather than light and is called the electron microscopy. In order to create an image, optical and electron microscopy involve light processes like reflection, refraction, diffraction or interaction of electron beam with the specimen. The third type of microscopy is scanning probe microscopy. In this type of microscopy to generate an image probes interact with the sample and involves the interaction of a scanning probe with the object's surface.

With the invention of scanning tunneling microscopes which are an instrument for imaging surface at atomic level scanning probe microscopy was founded in 1981 and is a sub-diffraction technique. Atomic force microscopy and scanning tunneling

microscopy are types of scanning probe microscopy. To scan the surface of an object all such methods use the contact of probe tip which is actually supposed to be flat. The image of scanning probe microscopes is formed by the combination of tip shape and topography of the sample. The probe must have a very sharp apex because resolution (i.e. how better we can distinguish two closely spaced points) of the microscope is defined by the apex of the probe. Sharper the probe, better the resolution.

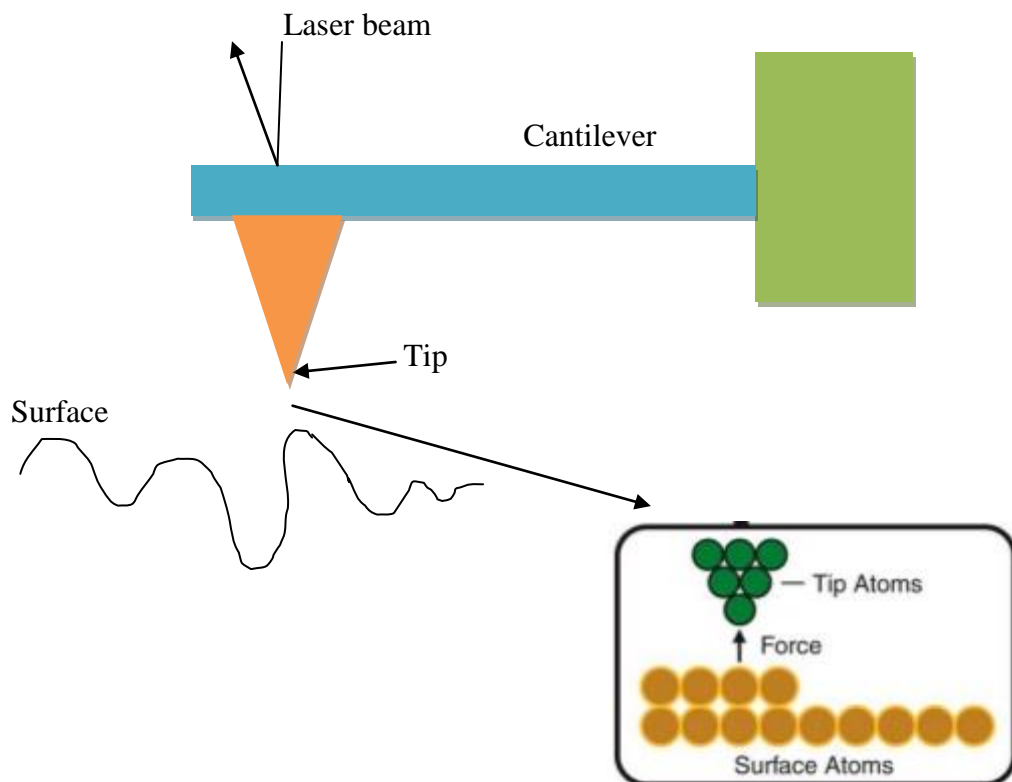


Figure 2.9 Scanning Probe Microscopy

(image concept:- [https:// www.slideshare.net/kajee01/atom-1](https://www.slideshare.net/kajee01/atom-1))

Resolution depends on wavelength of the light. Since the late 1940s X-ray microscopy has also been developed. To produce a magnified images of an object, X-ray microscopy uses electromagnetic radiation in soft band. X-ray microscopy reveals ‘soliton’ as a special type of magnetic wave:- a wave that can travel without resistance. To directly monitored a magnetic version of a soliton a powerful x-ray microscope was used. As they travel across a magnetic material, magnetic soliton control their shape and strength and are stable. Such magnetic wave can be used to

carry and store information in recent and more efficient form that generates less heat and requires less energy.

Soliton is a localized self similar structure and the motion of confined structures can be observed under the effects of externally applied gradients. The position of localized structure can be hold by the gradient. Localized structure's stable position depend on spatial gradients in the parameter of the system. Many non-homogenities can arise during the growing stages. To control the position of cavity soliton the non-homogenities such as system parameter variation can be used (4). Soliton force microscopy is the technique that not only permit to notice surface defects but also examine bulk defects in the device (5). Cavity soliton can scan a material both the surface and bulk. In Figure 2.10 a holding beam is paired with a VCSEL to provide the continuous power to generate cavity soliton. A better scheme for CS formation is frequency-selective feedback (FSF) element paired with a VCSEL.

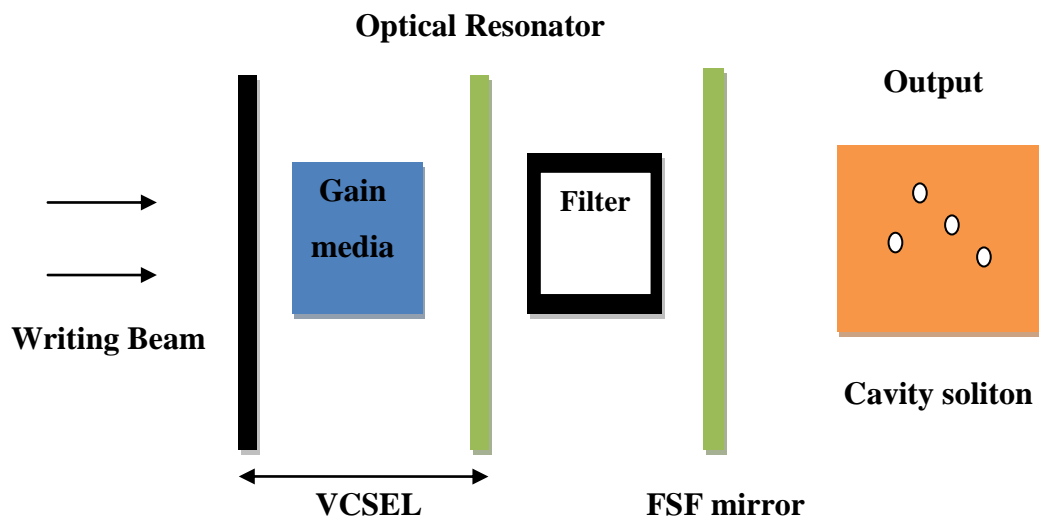


Figure 2.10 Scheme for CS generation in VCSEL coupled with frequency selective feedback

2.7 Methodology:

The governing equation for CS dynamics belongs to the family of perturbed NLSE (Non-Linear Schrödinger Equation) or CGLE (Complex Ginzburg-Landau

Equation). Both CGLE and NLSE nonlinear partial differential equation that donot lend them for analytic solutions in some case particularly for practical situation. A numerical approach is significant for solving such non-integrable perturbed NLSE or CGLE. Several numerical methods have been developed. Most of them can be classified into two broad categories known as ‘finite difference’ and ‘pseudospectral methods’. Split step fourier method is one of the method that has been used to solve the perturbed NLSE (34).

2.7.1 Split Step Fourier Method:

Split step fourier method is a pseudo-spectral numerical method. It is necessary to fourier transform because the linear step is made in the frequency domain while the nonlinear step is made in the time domain. Pseudospectral methods are faster than the general numerical method by up to an order of magnitude to achieve the same accuracy (35).

Consider the Nonlinear Schrödinger equation :-

$$\frac{\partial A}{\partial t} + i \frac{\beta_2}{2} \frac{\partial^2 A}{\partial x^2} - i\gamma |A|^2 A = Q \quad [2.7.1]$$

$$\frac{\partial A}{\partial t} = \left[-i \frac{\beta_2}{2} \frac{\partial^2}{\partial x^2} + i\gamma |A|^2 \right] A + Q \quad [2.7.2]$$

Where β_2 – group velocity diffraction parameter

γ – self-phase modulation parameter

Introducing linear and nonlinear operator as:-

$$\frac{\delta A}{\delta t} = (\hat{D} + \hat{N})A \quad [2.7.3]$$

$$\text{where } \hat{D} = -i \frac{\beta_2}{2} \frac{\delta^2}{\delta x^2} \quad (\text{linear operator})$$

$$\hat{N} = i\gamma |A|^2 \quad (\text{nonlinear operator})$$

\hat{D} is differential operator that represents in a linear medium the diffraction term and losses. \hat{N} is non-linear operator that accounts the effect of fibre nonlinearities on pulse propagation. In general, along the length of the fiber the diffraction and nonlinearity act together. The method obtains an approximate solution by assuming that the diffraction and nonlinear effects can be pretended to act independently in propagating the optical field over a small distance 'h'. In two steps the propagation from t to t+h is carried out (35).

In first step nonlinearity acts alone i.e. $\hat{D}=0$ in Eq[2.7.3]

$$\frac{\delta A}{\delta t} = \hat{N}A \quad [2.7.4]$$

By integrating from limit A(x,t) to A(x,t+h)

$$\int_{A(x,t)}^{A(x,t+h)} \frac{\delta A}{A} = \hat{N} \int_t^{t+h} \delta t$$

$$A(x,t+h) = A(x,t)\exp(hN) \quad [2.7.5]$$

In second step dispersion acts alone i.e. N=0 in Eq[2.7.3]

$$\frac{\delta A}{\delta t} = \hat{D}A$$

By integrating from limit A(x,t) to A(x,t+h)

$$\int_{A(x,t)}^{A(x,t+h)} \frac{\delta A}{A} = \hat{D} \int_t^{t+h} \delta t$$

$$A(x,t+h) = A(x,t)\exp(hD) \quad [2.7.6]$$

By combining first step and second step, the solution becomes:-

$$A(x,t+h) = \exp(hD)\exp(hN)A(x,t) \quad [2.7.7]$$

The operator $\exp(hN)$ as $\hat{N} = i\gamma|A|^2$ is easier to handle. In fourier domain operator $\exp(hD)$ is evaluated by replacing $\frac{\partial}{\partial t}$ by $-i\omega$ i.e. time domain is converted into frequency domain.

Exp(hD) is expressed as:-

$$\exp(hD) B(x,t) = F_T^{-1} \exp [h(D + N)] B(x,t)$$

$$\exp(hD) B(x,t) = F_T^{-1} \exp[hD(-i\omega)] F_T B(x,t) \quad [2.7.8]$$

The frequency in fourier domain is denoted by ω whereas F denotes the fourier transform. In split step fourier method the exact solution is given by:-

$$A(x,t+h) = \exp[h(D+N)] A(x,t) \quad [2.7.9]$$

Baker-Hausdorff formula is recalled for two (\hat{a} and \hat{b}) noncommuting operator $[\hat{a},\hat{b}] = ab-ba$

$$\text{Exp}(\hat{a})\text{Exp}(\hat{b}) = \exp(\hat{a}+\hat{b} + \frac{1}{2}[\hat{a},\hat{b}] + \frac{1}{12}[\hat{a}-\hat{b},[\hat{a},\hat{b}] + \dots\dots\dots)) \quad [2.8]$$

Using $\hat{a} = h\hat{D}$ and $\hat{b} = h\hat{N}$ the above equation is obtained. The nature of \hat{D} and \hat{N} operator is noncommutating. In step size h, the accuracy of split step fourier method holds to second order and can be improved by propagating the pulses from t to t+h over the one segment.

Eq.[2.7.7] becomes as:-

$$A(x,t+h) = \exp(\frac{h}{2}\hat{D}) \exp(\int_t^{t+h} N(t')dt') \exp(\frac{h}{2}\hat{D}) A(x,t) \quad [2.8.1]$$

Instead of at segment boundary the nonlinearity's effect is shown in the middle of the segment.

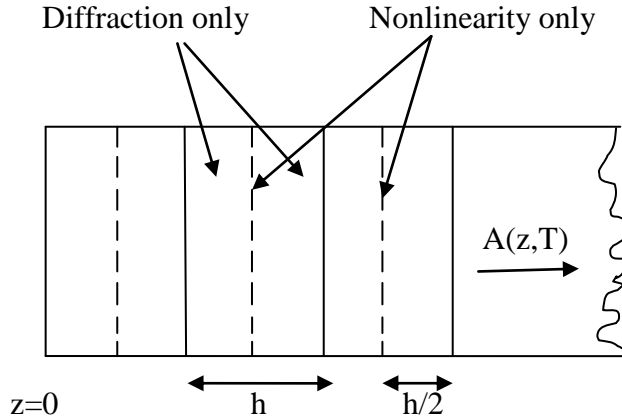


Figure 2.11 Schematic diagram of Symmetrized Split Step Fourier Method

Eq.[2.8.1] is symmetrized split step fourier method. The implementation of this method is relatively straightforward. Higher order version of this method proved to be useful in improving the computational efficiency. In optical fibre this method is used to study various nonlinear effects.

FLOW CHART OF SPLIT STEP FOURIER METHOD

Consider Non-linear Schrodinger Equation



$$\frac{\partial A}{\partial t} = (\hat{D} + \hat{N})A$$

In operator form



Diffraction (D) and nonlinear effect (N) act independently



When nonlinearity acts alone

$$\frac{\partial A}{\partial t} = \hat{N}A$$

When diffraction acts alone

$$\frac{\partial A}{\partial t} = \hat{D}A$$



Combining linear and nonlinear term

$$A(x, T+h) = \exp(hD)\exp(hN) A(x, T)$$



Combining for whole system

$$A(x, T+h) = \exp(h\hat{D})\exp(h\hat{N})\dots\dots\dots\exp(nh\hat{N})\exp(nh\hat{D})A(x, T)$$



Result

3.1 MATHEMATICAL MODELING

To generate or produce cavity soliton in VCSEL, various experimental demonstrations are utilized. Frequency selective feedback coupled with VCSEL is considered simpler and significant scheme for formation of cavity soliton. Saturable absorber also replaces the holding beam and produce losses. Thus, with this expectation that saturable absorber (SA) will create bistability of the cavity soliton and frequency selective feedback will compensate or counterbalance losses, the combined scheme of VCSEL with a saturable absorber paired with FSF (frequency selective feedback) was proposed. Because of the complex mathematical formulation, the study of cavity soliton has attracted growing interest. Mathematical modeling of cavity soliton involves the complex Ginzburg-Landau equation (CGLE) or perturbed nonlinear schrödinger equation (NLSE).

System consisting of a VCSEL with a saturable absorber and paired with FSF was considered. The cavity field $E(r,t)$ and the feedback field $F(r,t)$ in the model of mean-field cavity can be presented by the dynamical equations along with the rate equations of the feedback field and the carrier density for active and passive materials.

$$\frac{\partial E}{\partial t} = [-(1 - i\theta) + (1 - i\alpha)d_a + (1 - i\beta)d_p + i\Delta]E + F \quad [3.1]$$

$$\frac{\partial d_a}{\partial t} = c_1[d_a(1 + |E|^2) - \mu] \quad [3.2]$$

$$\frac{\partial d_p}{\partial t} = c_2[d_p(1 + s|E|^2) + \gamma] \quad [3.3]$$

$$\frac{\partial F}{\partial t} = -(\lambda + i\Omega_o)F + \sigma\lambda E \quad [3.4]$$

Here in the above equations, ‘ r ’ represents the transverse spatial coordinate and ‘ t ’ is the time normalized to the cavity round-trip period. On the right hand side of Eq.[3.1] the first term describes the linear losses incurred by the system. The ‘1’ is the normalized cavity loss and ‘ θ ’ is the mistuning between the frequencies of the feedback field and the cavity that measures the mismatch between the feedback and the cavity frequencies. In order to reduce the linear losses θ needs to be small. ‘ μ ’ represents the pump parameter and ‘ α ’ denote the linewidth enhancement factor for the active materials while those for passive materials are given by ‘ γ ’ and ‘ β ’ respectively. α and β possess positive and large values usually for VCSEL. The second and third terms on the right hand side of Eq.[3.1] represent carrier densities. The carrier densities in active medium is represented by d_a and in passive medium it is represented by d_p . The fourth term represents the diffraction operator for a D-dimensional system with $\Delta = r^{(1-D)} \frac{\partial}{\partial r} (r^{(D-1)} \frac{\partial}{\partial r})$ being the transverse Laplacian. c_1 and c_2 are the ratio of the photon lifetime to the carrier lifetime in the active and passive materials respectively. FSF is provided by a DBR. In the Eq.[3.4] σ represents the feedback strength that needs to be positive so as to provide gain in the cavity and it assumes a value between 0 and 1. The frequency selection of the feedback is accomplished by a filter and λ represents the bandwidth of the filter reflection. The resonance frequency of the feedback field is denoted by Ω_0 . Numerical method should be solved to understand the effects caused by nonlinearity in VCSEL. For the stability and existence of the cavity solitons, the direct numerical analysis based on the split step fourier method of the governing equations display matching results. By introducing a phase gradient all optical control on CS’s has been demonstrated (6).

3.2 CS generation and dynamics with variation of pump power (μ) for active material

In earlier studies CS was found for a fixed pump parameter for active material (μ). In current case we study the gradient in the pump parameter. At the centre of cross-sectional area of VCSEL, μ (pump power) is fixed. But as it goes off-axis, μ parameter shows variation. We use different gradient function.

CS dynamics for Sin(r) gradient function:-

We considered a gradient function of the form of Sin(r) where ‘r’ is the radius of the cross-sectional area of VCSEL. Taking saturation parameter “s=10”. The pump power for active material (μ) consists of two parts. As shown in Fig 3.1 (a) $\mu=1.365+0.015\sin(r)$, the first part is fixed value or constant gradient whereas the second part consist of periodic modulation of parameter. CS was formed in the form of the multiple number of branches and variation in these branches were observed. And as the perturbation increases from 0.01 to 0.035 the distance between the branches increases. Branch on the positive axis start moving away from zero point. Fig.3.1 (d) shows the plot between the distance of CS and perturbation applied. At 0.04 modulation the decay was observed.

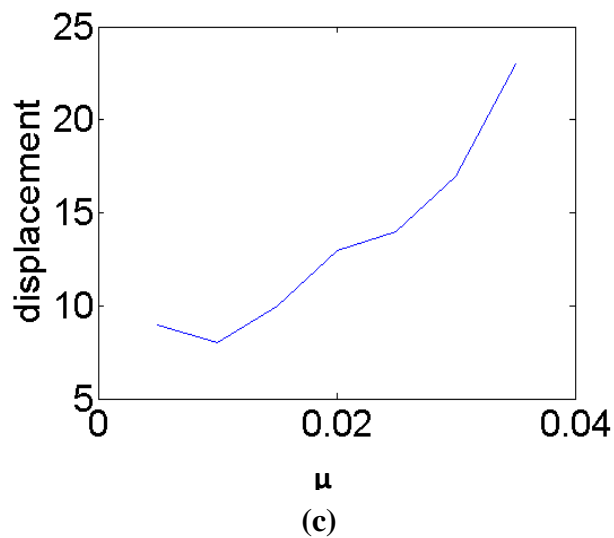
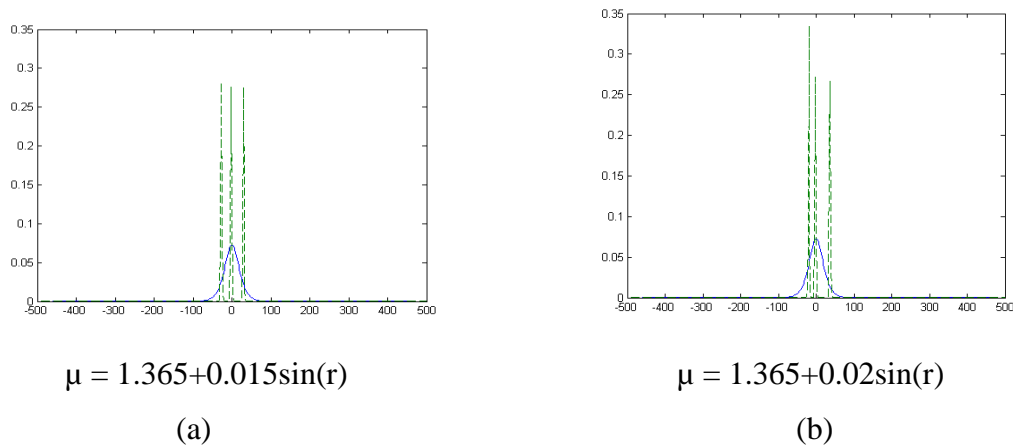


Figure 3.1 Variation of pump parameter μ for Sin(r) gradient function

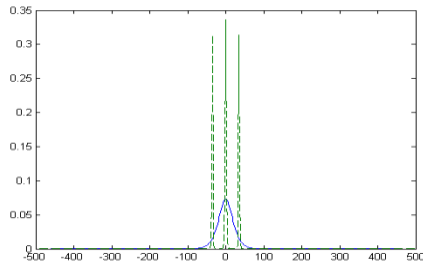
(a) $\mu = 1.365+0.015 \text{ Sin}(r)$

(b) $\mu = 1.365+ 0.02 \text{ Sin}(r)$

(c) plot of displacement of CS and modulation of parameter

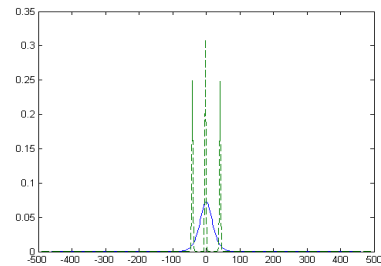
CS dynamics for cos(r) gradient function:-

In this case, with saturation parameter $s=10$, we consider the gradient function of the form of $\text{Cos}(r)$. 'r' being the radius of cross-sectional area of VCSEL. CS were formed in the form of the branches. Variation in movement of branches is observed. The branches expand firstly and then contract as perturbation increases. The number of branches decreases as approximation increases. Also difference in amplitude was observed. At 0.55 modulation the decay was noticed.



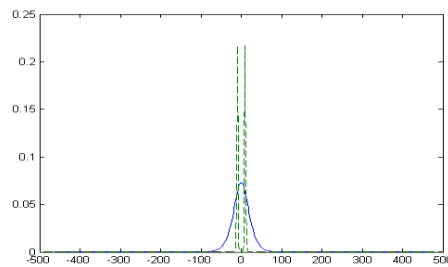
$$\mu = 1.365 + 0.01 \cos(r)$$

(a)



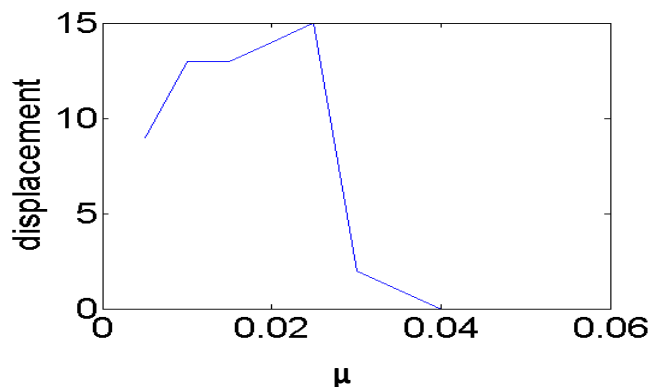
$$\mu = 1.365 + 0.025 \cos(r)$$

(b)



$$\mu = 1.365 + 0.035 \cos(r)$$

(c)



(d)

Figure 3.2 Variation of μ pump parameter for $\text{cos}(r)$ gradient function

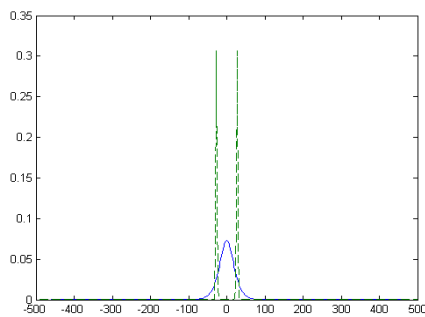
(a) $\mu = 1.365 + 0.01 \text{Cos}(r)$

(b) $\mu = 1.365 + 0.025 \text{Cos}(r)$

(c) $\mu = 1.365 + 0.035 \text{Cos}(r)$ and (d) plot of displacement of CS and perturbation

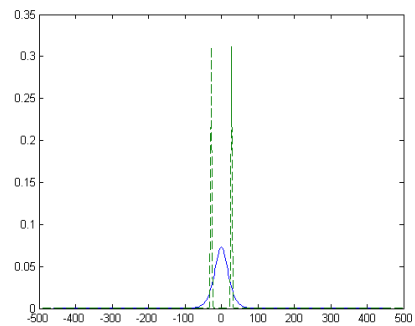
Dynamics of CS for $f(r)=r$ linear gradient function:-

Here, we considered the linear gradient function i.e. $f(r)=r$ using saturation parameter $s = 10$. CS is generated in the form of two branches. As gradient function increases the number of branches of cavity soliton remain same throughout with the same amplitude but show variation in movements. Firstly, the displacement remain constant but at 0.00005 shows sudden expansion. By applying 0.00006 branches contract and later on as gradient functions increases, the branches started moving close to zero point. Decay was seen at 0.00025.



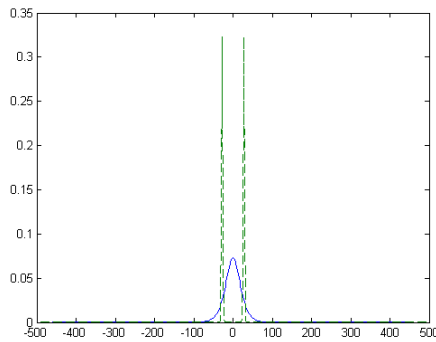
$$\mu = 1.365 + \text{abs}(0.00001r)$$

(a)



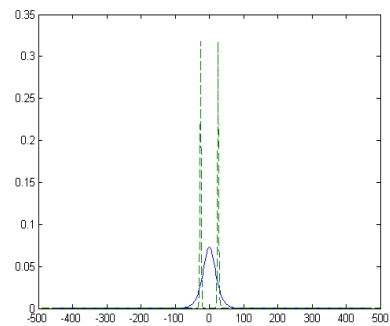
$$\mu = 1.365 + \text{abs}(0.00003r)$$

(b)



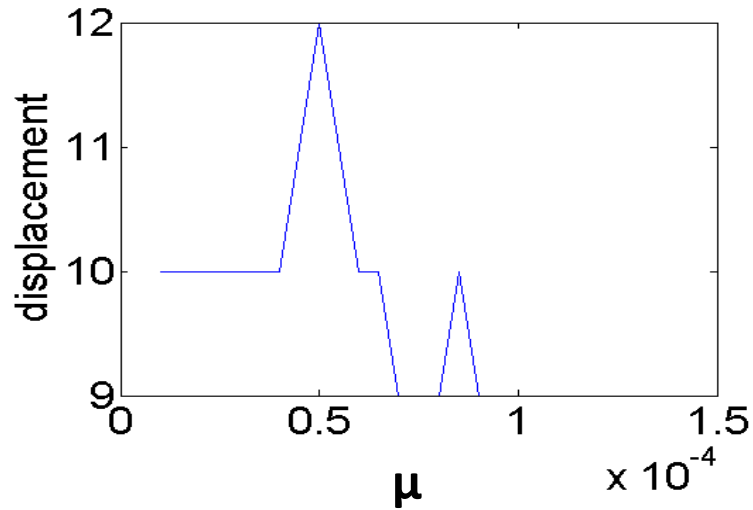
$$\mu = 1.365 + \text{abs}(0.00006r)$$

(c)



$$\mu = 1.365 + \text{abs}(0.000085r)$$

(d)

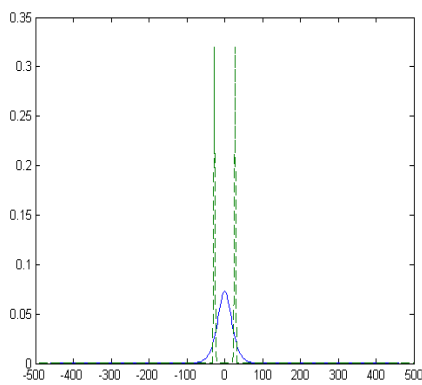


(e)

Figure 3.3(a) to (d) variation of μ pump parameter for linear gradient function $f(r)=r$ and (e) plot of modulation of gradient function and displacement

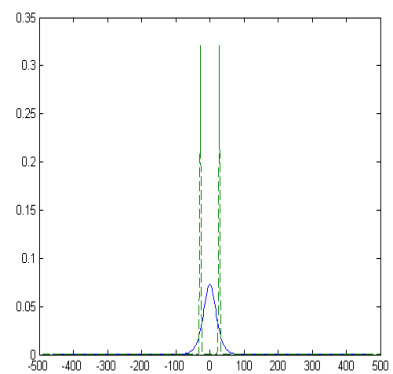
CS dynamics for r^2 gradient function:-

We consider a gradient function of the form of r^2 . Here in this case no such variation is observed in displacement, in number of branches, in amplitude. Both the branches remain equally spaced as perturbation is increased. The “two” branches show the constant movement towards the zero point. At 0.00000045 decay was seen.



$$\mu = 1.365 + \text{abs}(0.0000001r^2)$$

(a)



$$\mu = 1.365 + (0.00000035r^2)$$

(b)

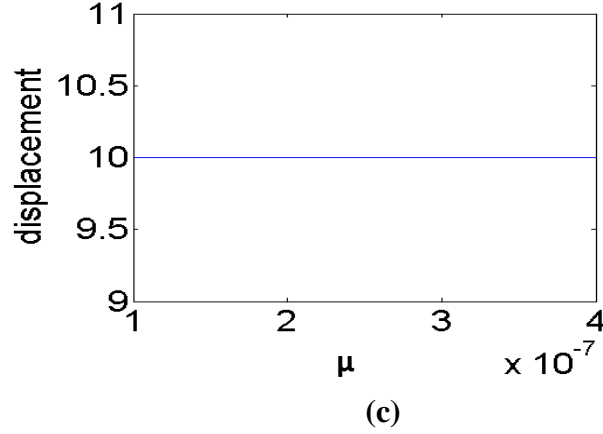


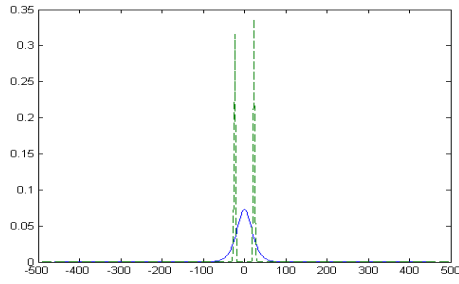
Figure 3.4(a)(b) variation of μ pump parameter for r^2 gradient function and (c) displacement of CS Vs perturbation plot

3.3 Formation and dynamics of CS with variation of ‘ γ ’ pump parameter for passive material

As discussed above that CS was found for a fixed pump parameter in earlier studies but in current case we study the gradient in pump parameter for a passive material. At the centre of the cross-sectional area of VCSEL, pump parameter for passive material ‘ γ ’ is constant with value 0.5. But off axis γ parameter same as μ parameter shows variation by using different gradient functions such as $\sin(r)$, $\cos(r)$, r and r^2 .

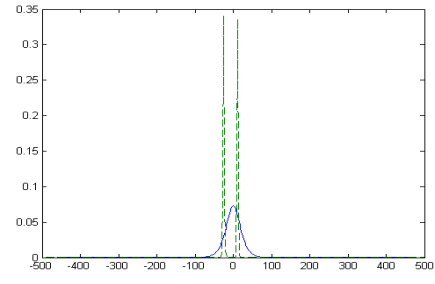
CS dynamics for $\sin(r)$ function:-

Taking saturation parameter (s) = 10 we consider a gradient function of the form of $\sin(r)$ where ‘ r ’ is radius of cross-sectional area of VCSEL. The pump parameter for passive material ‘ γ ’ consist of two parts as shown below in Fig.3.5 (a) $\gamma=0.5+0.01\sin(r)$. The first part of γ is constant gradient and second part is periodic modulation of parameters. The CS is formed in the form of multiple branches and show variation in movements of branches. The branch on positive side moves towards zero point and negative side started moving away from zero point. Except at 0.025 and 0.045 perturbation both the branches on positive and negative axis move towards zero point. At 0.15 modulation the decay was observed.



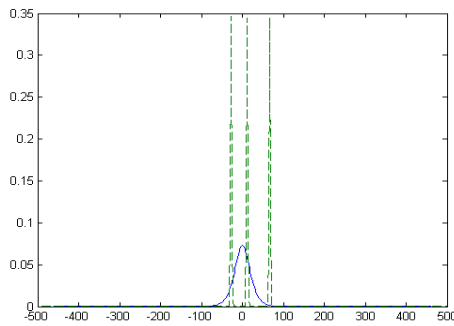
$$\gamma = 0.5 + 0.01\sin(r)$$

(a)



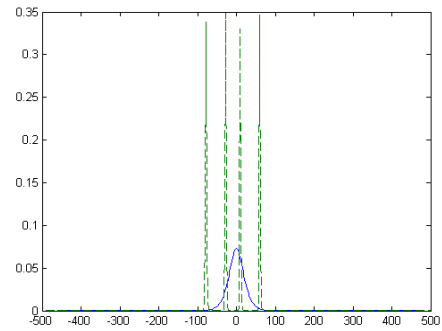
$$\gamma = 0.5 + 0.04\sin(r)$$

(b)



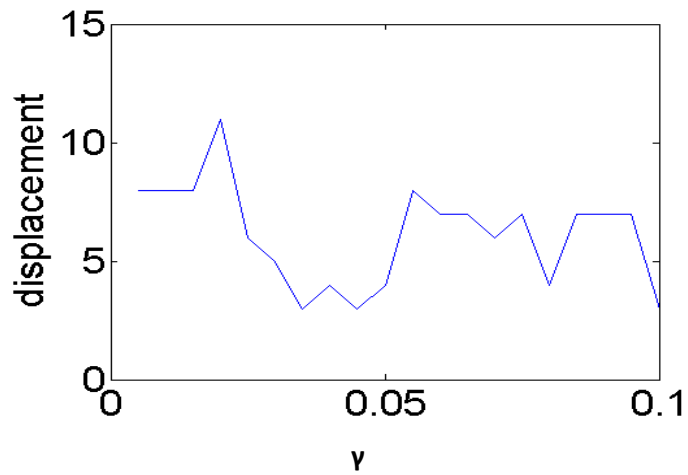
$$\gamma = 0.5 + 0.08\sin(r)$$

(c)



$$\gamma = 0.5 + 0.1\sin(r)$$

(d)



(e)

Figure 3.5 Variation of pump parameter γ for $\sin(r)$ gradient function

(a) $\gamma=0.5+0.01\sin(r)$

(b) $\gamma=0.5+0.04\sin(r)$

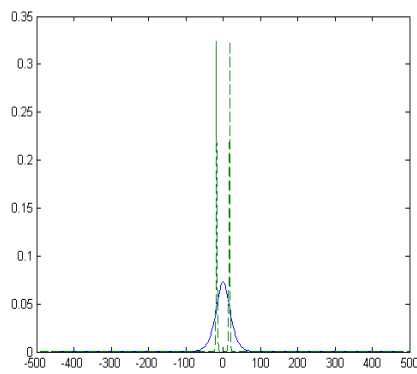
(c) $\gamma=0.5+0.08\sin(r)$

(d) $\gamma=0.5+0.1\sin(r)$

(e) plot between displacement of CS and perturbation

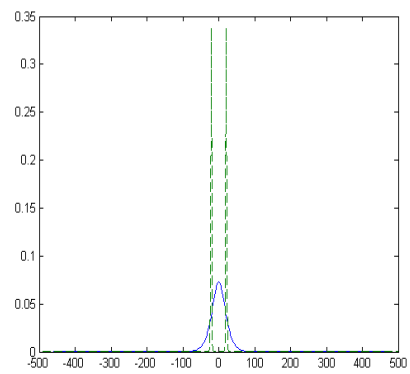
Dynamics of CS for $\cos(r)$ gradient:-

We consider the gradient function of the form of $\cos(r)$, r being the radius of cross-sectional area of VCSEL. Taking saturation parameter $s=10$, the CS is formed in the form of ‘two’ to ‘four’ branches by the modulation of parameter. The branches show expansion in the movement from zero point but later as perturbation increases the movement remain constant. At 0.07 shows huge expansion (move away from zero point). From 0.08 to 0.1 the branches contract (i.e. move towards zero point). The decay was noticed at 0.15.



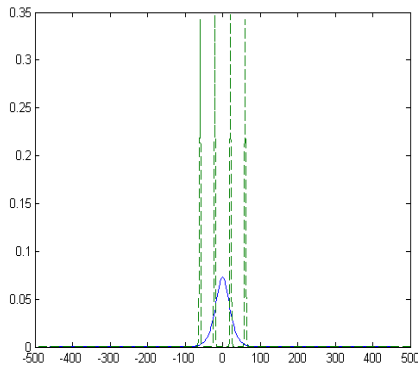
$$\gamma = 0.5 + 0.01 \cos(r)$$

(a)



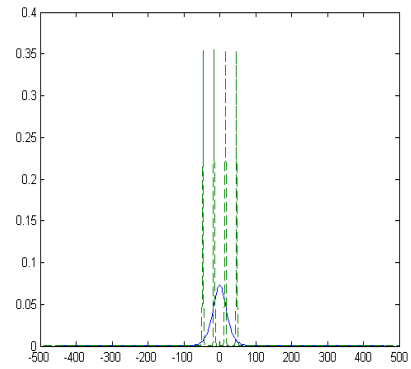
$$\gamma = 0.5 + 0.04 \cos(r)$$

(b)



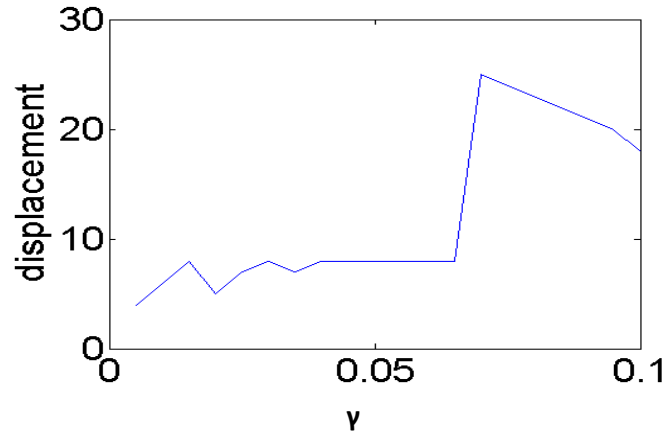
$$\gamma = 0.5 + 0.08 \cos(r)$$

(c)



$$\gamma = 0.5 + 0.1 \cos(r)$$

(d)



(e)

Figure 3.6 Variation of pump parameter γ for $\cos(r)$ gradient function

(a) $\gamma=0.5+0.01\cos(r)$

(b) $\gamma=0.5+0.04\cos(r)$

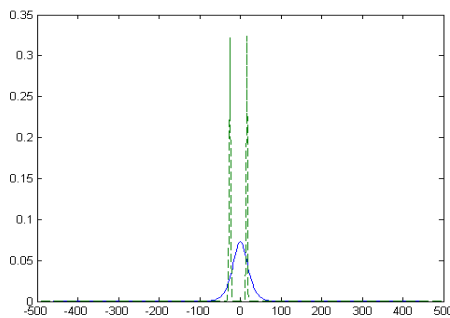
(c) $\gamma=0.5+0.08\cos(r)$

(d) $\gamma=0.5+0.1\cos(r)$

(e) plot between displacement of CS and perturbation

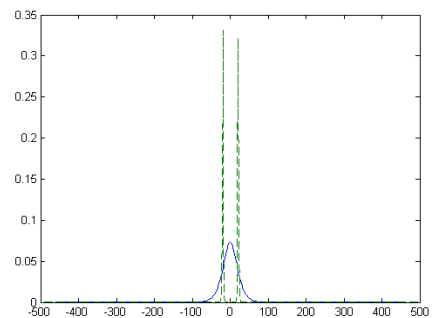
CS dynamics for $f(r)=r$ linear gradient function:-

Here, we considered the linear gradient function i.e. $f(r)=r$ using saturation parameter $s = 10$. CS is generated in the form of multiple branches. From 0.00001 to 0.000035 “two” branches are formed and from 0.00004 to 0.000085 “three” branches. Show huge variations in distance. On applying the 0.00002 approximation ‘two’ branches expand till 0.00004. Later as perturbation increases the branches contract whereas few expand. At 0.00008 sudden contractions (branches move close to zero point) was observed. At 0.0002 perturbation decay was seen.



$\gamma= 0.5+0.00001r$

(a)



$\gamma= 0.5+0.00003r$

(b)

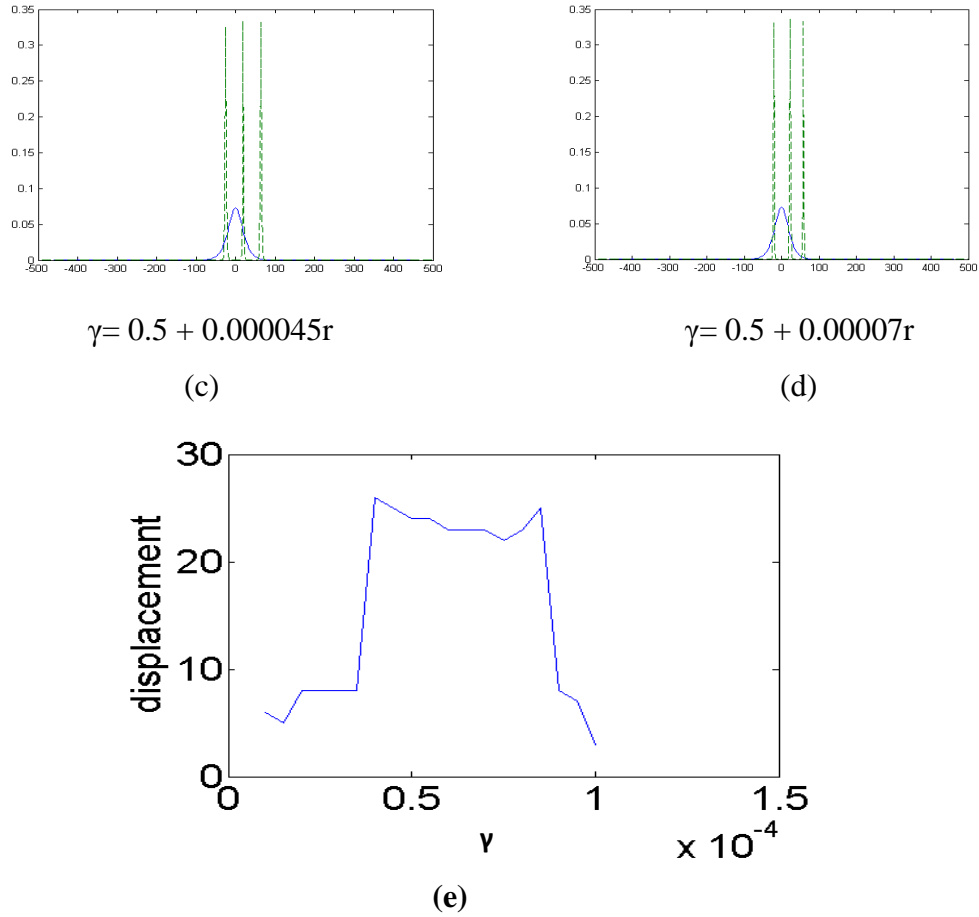
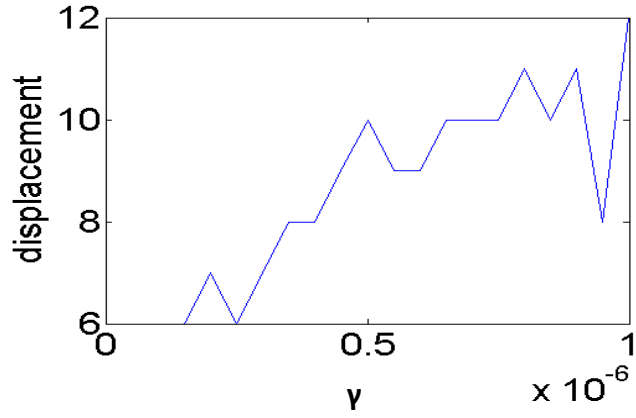


Figure 3.7 Variation of pump parameter γ for r linear gradient function

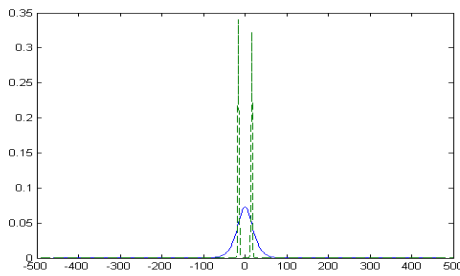
- (a) $\gamma = 0.5 + 0.00001r$ (b) $\gamma = 0.5 + 0.00003r$
 (c) $\gamma = 0.5 + 0.000045r$ (d) $\gamma = 0.5 + 0.00007r$
 (e) plot between displacement of CS and perturbation

Dynamics of CS for r^2 gradient function:-

We consider a gradient function of the form of r^2 . CS are formed in the form of multiple branches. Vast variation in movement of branches of cavity soliton was monitored. At 0.0000002 both the branches move away from zero point i.e. shows expansion. At 0.00000025 the branches contract and later go on expanding with increasing disturbance. At 0.00000055 again both the branches come close to zero point. Numbers of branches remain 2 by increasing approximation.

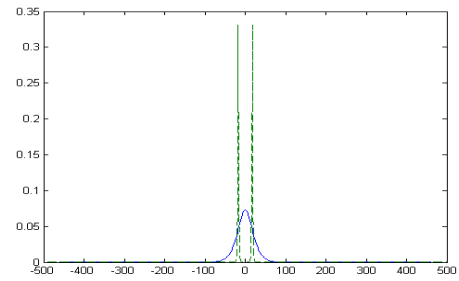


(a)



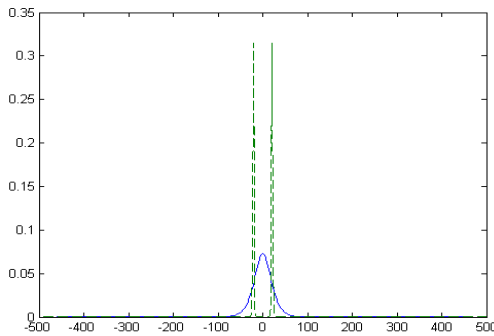
$$\gamma = 0.5 + 0.0000001r^2$$

(b)



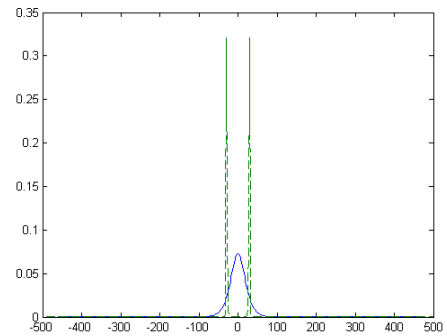
$$\gamma = 0.5 + 0.0000002r^2$$

(c)



$$\gamma = 0.5 + 0.00000035r^2$$

(d)



$$\gamma = 0.5 + 0.0000008r^2$$

(e)

Figure 3.8(a) plot of displacement of CS and perturbation

(b) $\gamma = 0.5 + 0.0000001r^2$

(c) $\gamma = 0.5 + 0.0000002r^2$

(d) $\gamma = 0.5 + 0.00000035r^2$

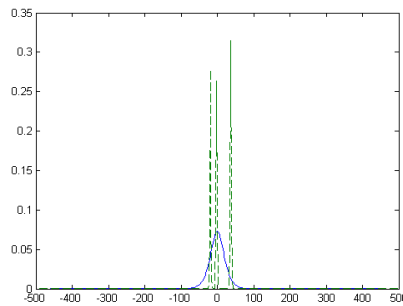
(e) $\gamma = 0.5 + 0.0000008r^2$

3.4 CS generation and dynamics with variation of μ pump parameter for active materials

Till now we varied only one parameter keeping “s” saturation parameter constant. Now we investigate the same with non-constant gradient or ‘s’ where $s=10+0.01\sin(r)$. As periodic modulation of parameter varies the saturation parameter also varies. We studied the gradient in pump parameter for active materials (μ). At the centre of cross-sectional area of VCSEL, μ is fixed. But as it goes off axis, μ pump power shows variation. We use different gradient.

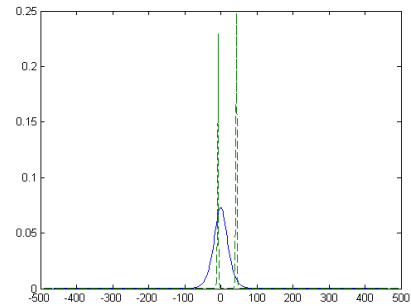
CS dynamics for $\sin(r)$ gradient function:-

We considered a gradient function of the form of $\sin(r)$ where r is the radius of cross-sectional area of VCSEL. μ (pump parameter) consist of two parts. The first part of μ is constant gradient and second part is periodic modulation of parameters. Taking $s=10+0.01\sin(r)$ where ‘s’ is saturation parameter. The CS is formed in the form of multiple branches. The movement of cavity soliton show expansion as perturbation increases except the case when the perturbation $0.015\sin(x)$ is applied. The decay was observed at perturbation $0.04\sin(x)$.



$$\mu = 1.365 + 0.02\sin(r)$$

(a)



$$\mu = 1.365 + 0.03\sin(r)$$

(b)

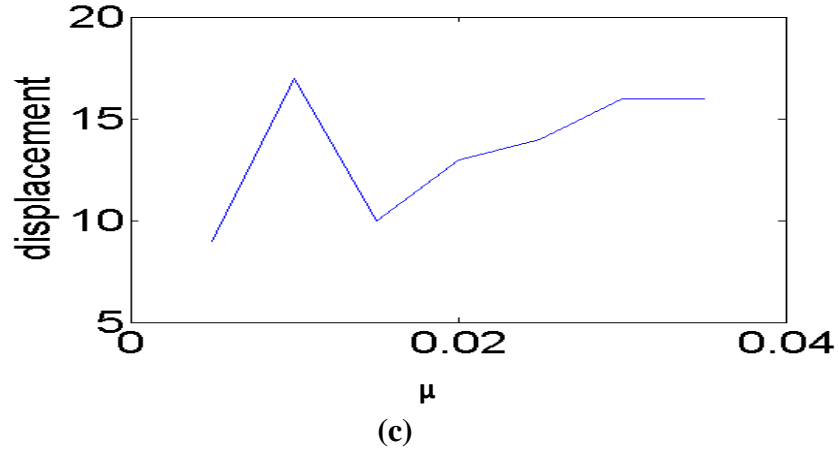


Figure 3.9 Variation of μ pump parameter for $\sin(r)$ function

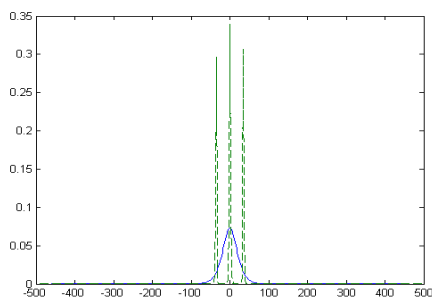
(a) $\mu = 1.365 + 0.02 \sin(r)$

(b) $\mu = 1.365 + 0.03 \sin(r)$

(c) perturbation and displacement of CS plot

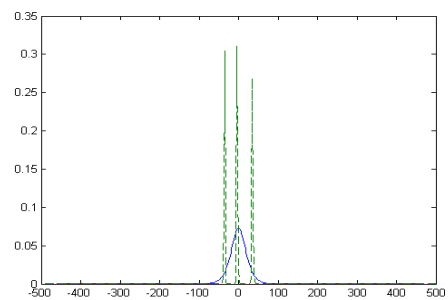
CS dynamics for $\cos(r)$ gradient function:-

We consider the gradient function of the form of $\cos(r)$, r being the radius of cross-sectional area of VCSEL. Taking saturation parameter $s = 10 + 0.01 \sin(r)$, the CS is formed in the form of multiple branches by the modulation of parameter. At 0.005 perturbation ‘2’ branches are formed but as perturbation increases from 0.01 to 0.025 ‘3’ branches were observed. By providing more modulation the number of branches decreases from ‘3’ to ‘1’. Along with the variation in branches of cavity soliton, the movement of branches also differ. Mostly the expansion is seen except at 0.015 where the branches contract. At 0.03 “one” branch is formed at zero point. Fig.3.10 describes the variation in μ parameter using the $\cos(x)$ function.



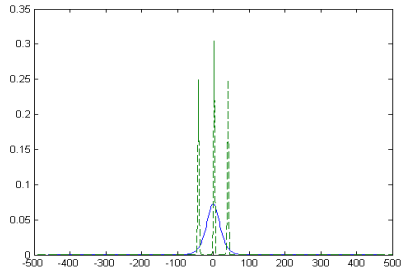
$\mu = 1.365 + 0.01 \cos(r)$

(a)



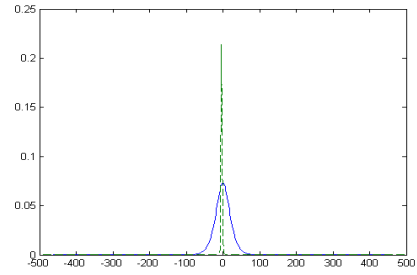
$\mu = 1.365 + 0.02 \cos(r)$

(b)



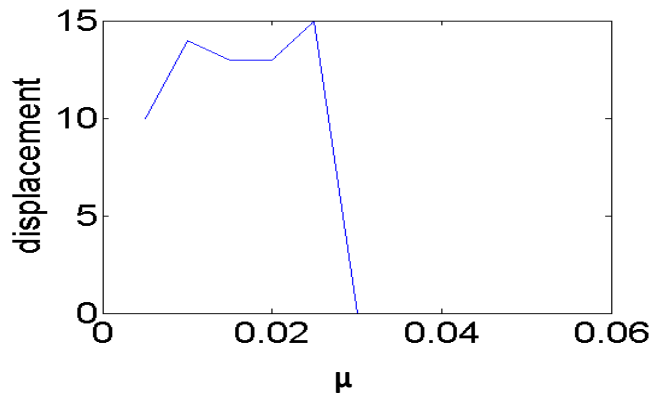
$$\mu = 1.365 + 0.025 \cos(r)$$

(c)



$$\mu = 1.365 + 0.04 \cos(r)$$

(d)



(e)

Figure 3.10 Variation in μ pump parameter for $\cos(r)$ periodic gradient function

(a) $\mu = 1.365 + 0.01 \cos(r)$

(b) $\mu = 1.365 + 0.02 \cos(r)$

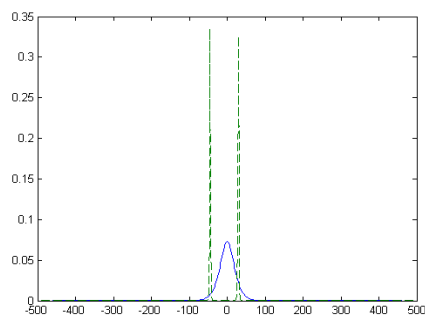
(c) $\mu = 1.365 + 0.025 \cos(r)$

(d) $\mu = 1.365 + 0.04 \cos(r)$

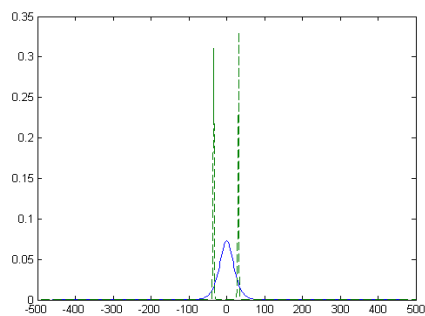
(e) perturbation Vs displacement of CS plot

CS dynamics for $f(r)=r$ linear gradient function:-

Here, we considered the linear gradient function i.e. $f(r)=r$ using saturation parameter $s = 10 + 0.01 \sin(r)$. CS is generated in the form of two branches. Number of branches remain same. By applying 0.0002 perturbation the branches expands. Branch on negative side move towards zero point and branch on positive side move away from zero point.



$$\mu = 1.365 + 0.00015r$$



$$\mu = 1.365 + 0.0002r$$

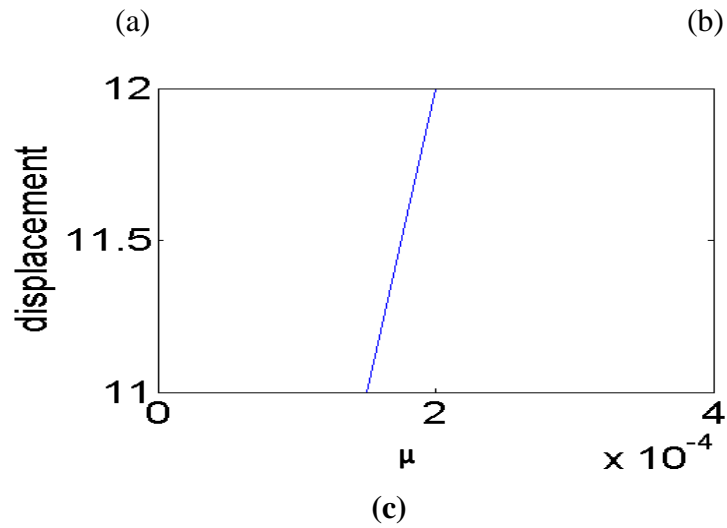


Figure 3.11 Variation of μ pump parameter for r linear gradient function

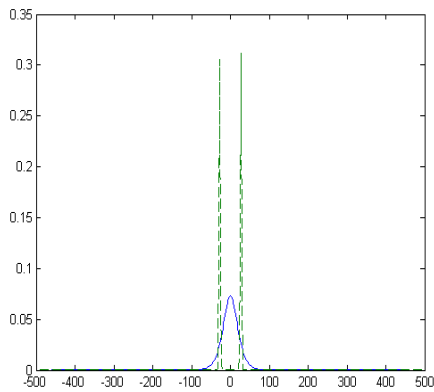
(a) $\mu=1.365+0.00015r$

(b) $\mu=1.365+0.0002r$

(c) perturbation Vs displacement of CS plot

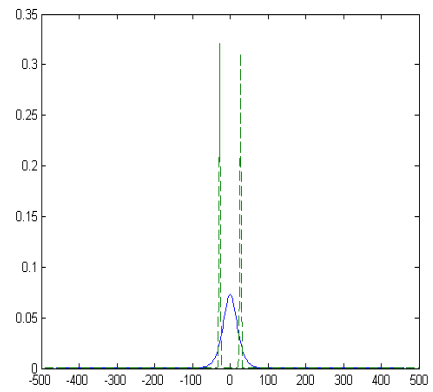
cavity soliton dynamics for r^2 gradient function:-

We consider a gradient function of the form of r^2 . CS are formed in the form of multiple branches. No change in movement of branches is observed. Both the branches of different amplitude remain equally spaced.



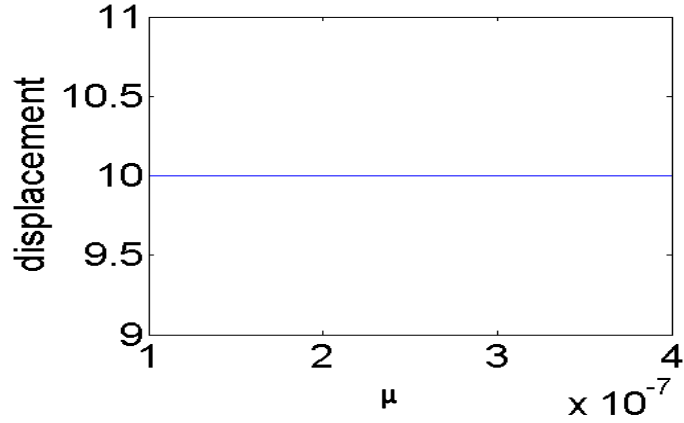
$\mu= 1.365+0.0000001r^2$

(a)



$\mu= 1.365+0.00000025r^2$

(b)



(c)

Figure 3.12 Variation of μ pump parameter r^2 gradient function

(a) $\mu=1.365+0.0000001r^2$ (b) $\mu=1.365+0.00000025r^2$

(c) plot between displacement and perturbation

3.5 Formation and dynamics of CS with variation of γ pump parameter for passive materials

We study the gradient in pump parameter γ for passive material. At the centre of cross-sectional area of VCSEL, γ is fixed. But as it goes off-axis, γ pump parameter shows variation. We use different gradient function.

CS dynamics for $\sin(r)$ periodic gradient function:-

We considered a gradient function of the form of $\sin(r)$ where r is the radius of cross-sectional area of VCSEL. with saturation parameter $s=10+0.01\sin(r)$, γ (pump parameter) consist of two parts. The first part of γ is constant gradient and second part is periodic modulation of parameters. The CS is formed in the form of multiple branches. The movement of branches shows three types of variation. Firstly it remain constant even after applying some perturbation. Then, later on as perturbation increases it contract and then suddenly at 0.08 perturbation the branches move away from zero point. The second branch on positive side start moving away from the zero point at 0.08 whereas from 0.085 to 0.095 branches contract again. The decay was monitored at 0.15.

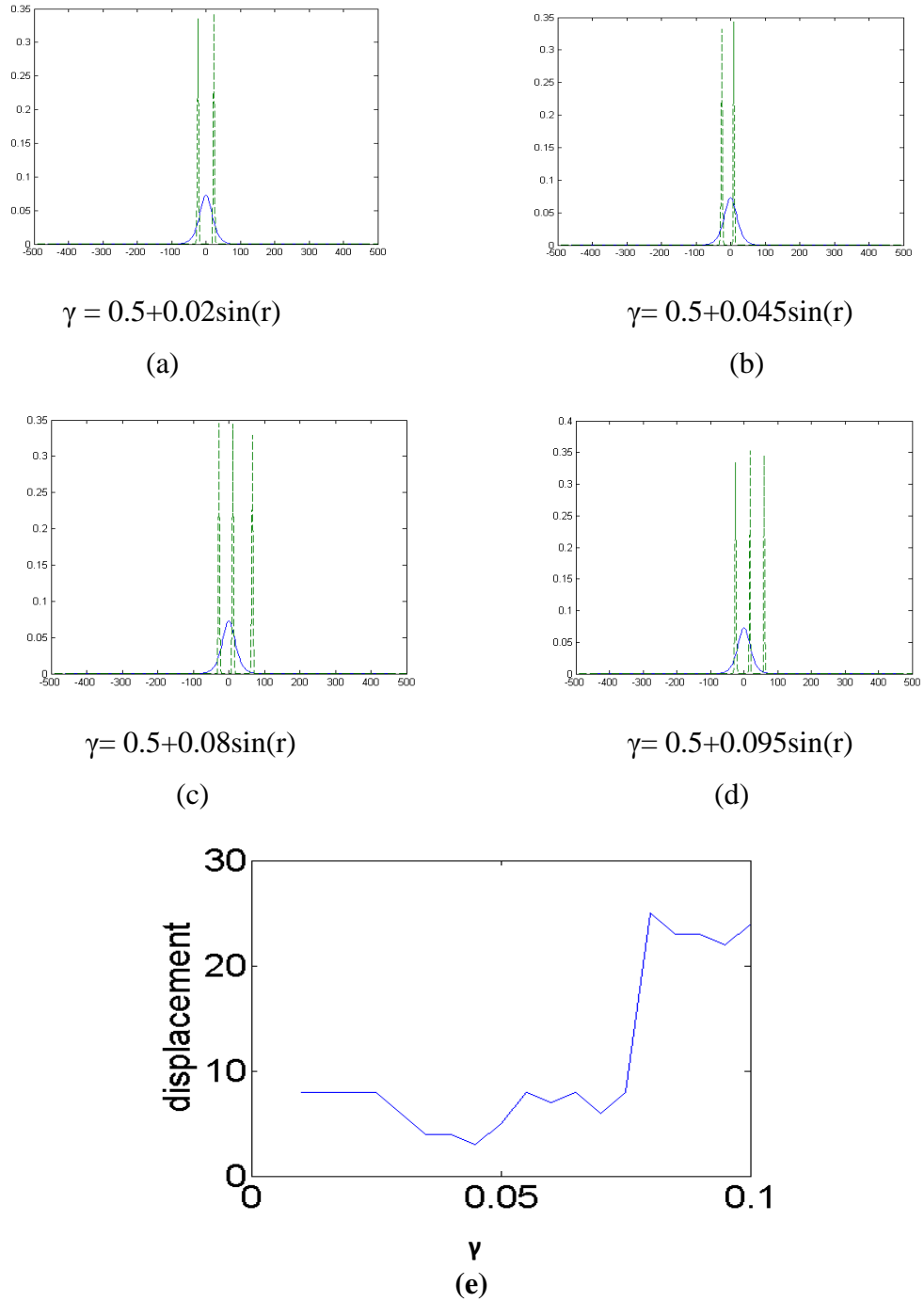


Figure 3.13 Variation of γ pump parameter for $\sin(r)$ gradient function

(a) $\gamma = 0.5 + 0.02 \sin(r)$ (b) $\gamma = 0.5 + 0.045 \sin(r)$

(c) $\gamma = 0.5 + 0.08 \sin(r)$ (d) $\gamma = 0.5 + 0.095 \sin(r)$

(e) perturbation Vs displacement of CS plot

CS dynamics for $\cos(r)$ function:-

We consider the gradient function of the form of $\cos(r)$, r being the radius of cross-sectional area of VCSEL. Taking saturation parameter $s = 10 + 0.01 \sin(r)$, the CS is formed in the form of multiple branches by the modulation of parameter. As

perturbation increases the movement of the branches show fluctuation. It first contracts at 0.025 and 0.035 and then from 0.04 to 0.06 perturbation no variation in movement is monitored. As approximation 0.065 is applied it expands and then again as perturbation increases branches starts contracting. Decay was observed at $0.15\cos(r)$.

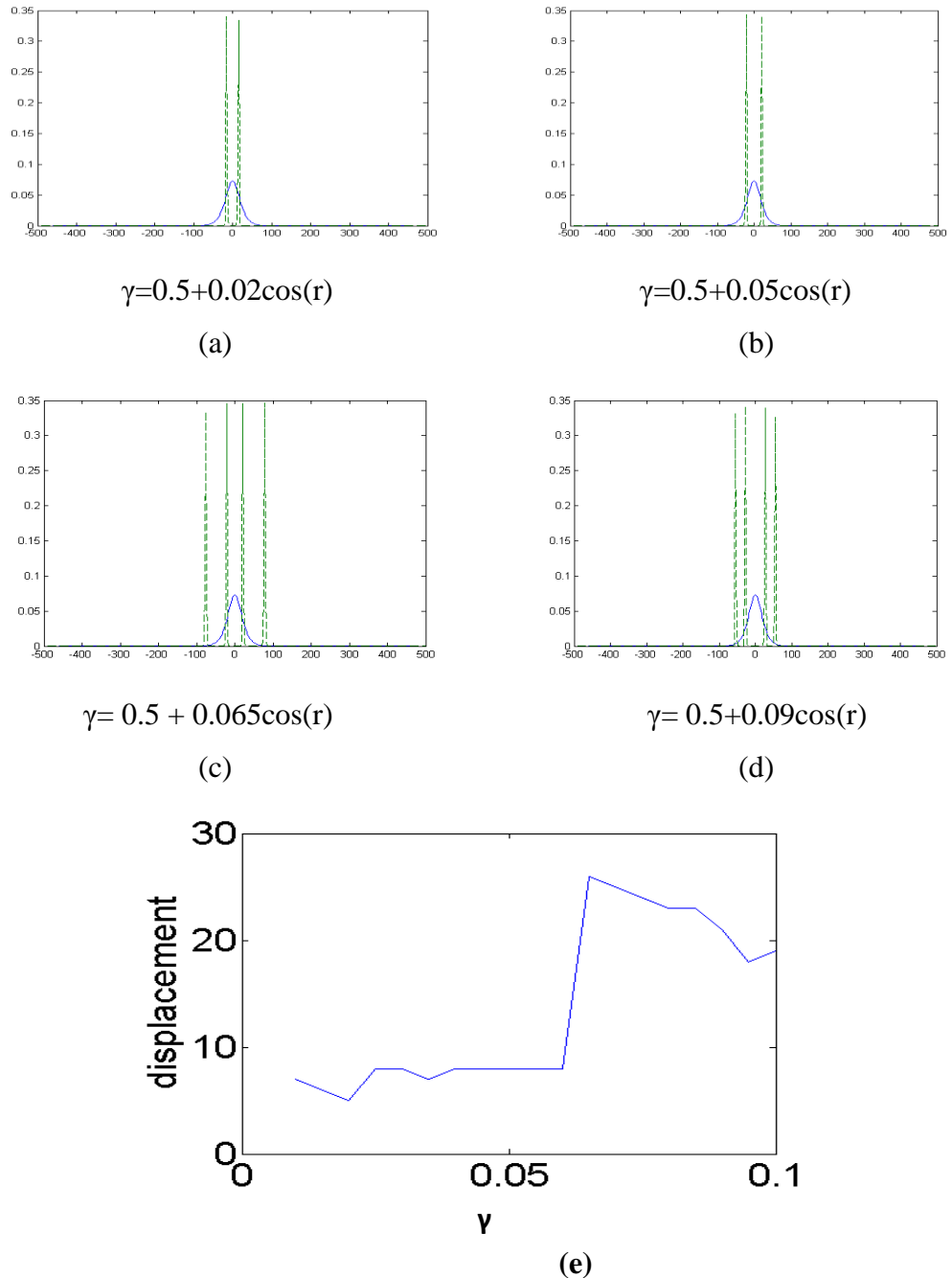


Figure 3.14 Variation of γ pump parameter for $\cos(r)$ gradient function

(a) $\gamma = 0.5 + 0.02\cos(r)$

(b) $\gamma = 0.5 + 0.05\cos(r)$

(c) $\gamma = 0.5 + 0.065\cos(r)$

(d) $\gamma = 0.5 + 0.09\cos(r)$

(e) plot between perturbation and displacement of CS

CS dynamics for $f(r)=r$ gradient function:-

Here, we considered the linear gradient function i.e. $f(r)=r$ using saturation parameter $s = 10+0.01\sin(r)$. CS is generated in the form of multiple branches. At 0.000015 the branches move towards zero point and then expand from 0.00002 to 0.00004. Further as approximation increases branches mostly show expansion (move away from zero point) expect when 0.000045, 0.000055, 0.00008 and 0.000085 perturbation is applied. Decay was observed at 0.0002.

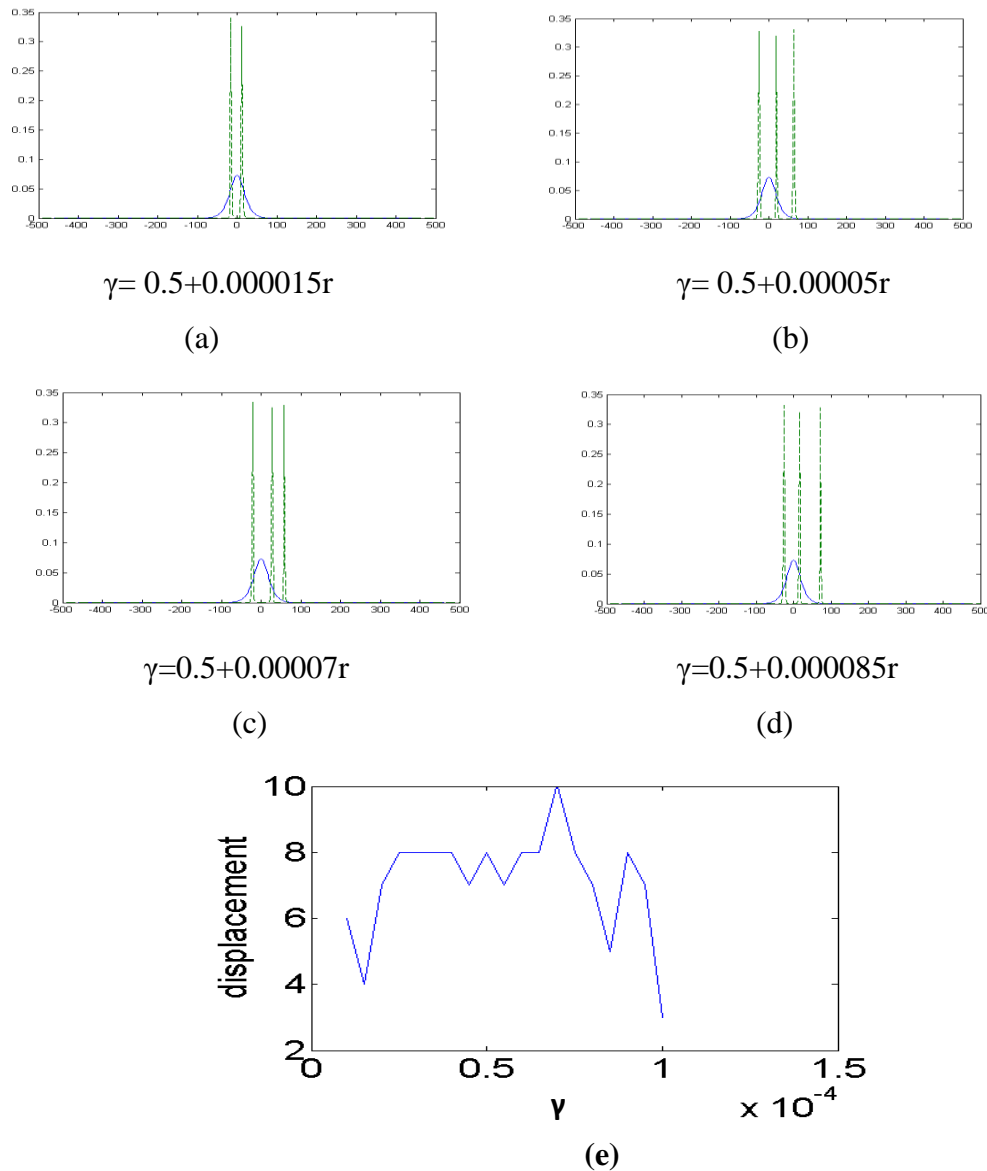


Fig 3.15 Variation of γ pump parameter for r linear gradient function

- (a) $\gamma = 0.5 + 0.000015r$ (b) $\gamma = 0.5 + 0.00005r$
- (c) $\gamma = 0.5 + 0.00007r$ (d) $\gamma = 0.5 + 0.000085r$
- (e) plot between perturbation and displacement of CS

CS dynamics for r^2 gradient function:-

We consider a gradient function of the form of r^2 . CS are formed in the form of multiple branches with saturation parameter $s=10+0.01\sin(r)$. Huge fluctuation is observed in this case. The CS on positive axis move away from zero point except when $0.00000045r^2$, $0.00000055r^2$, $0.00000075r^2$ and $0.00000095r^2$ perturbation is applied the branches move slightly towards the zero point (contract).

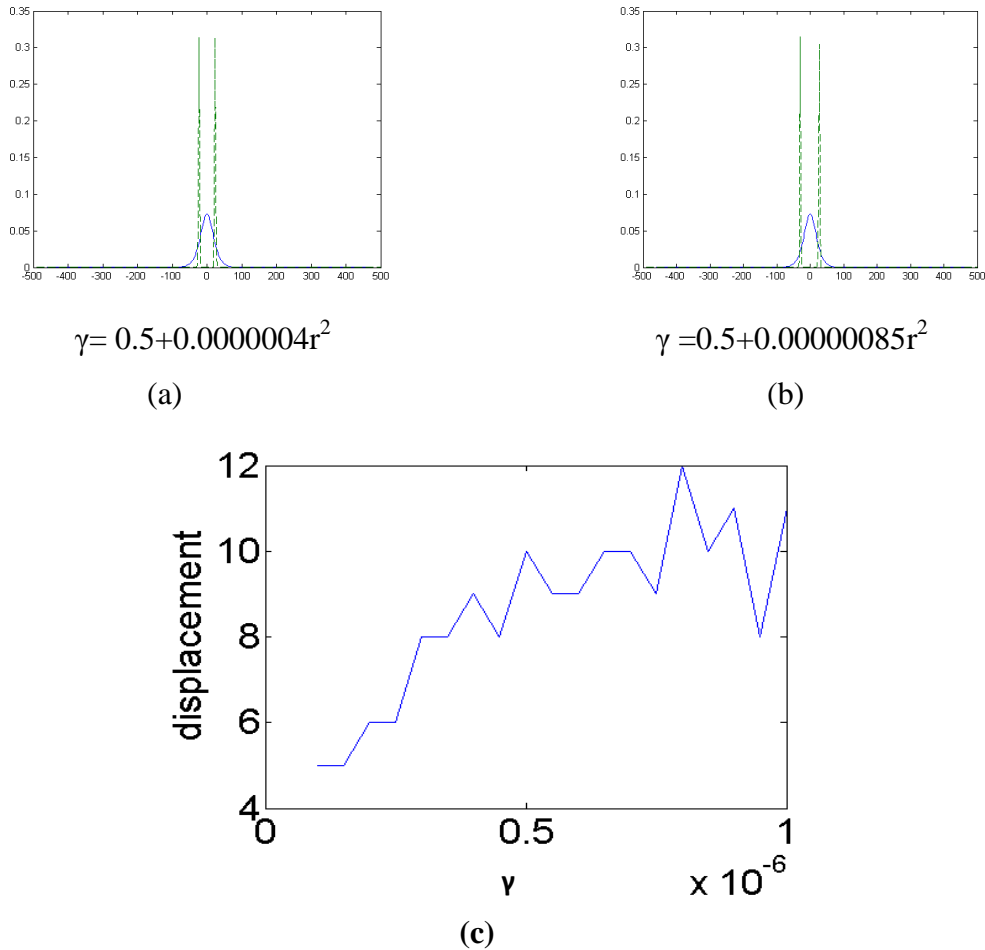


Figure 3.16 Variation of γ pump parameter using r^2 gradient function

(a) $\gamma = 0.5 + 0.0000004r^2$ (b) $\gamma = 0.5 + 0.00000085r^2$

(c) plot between displacement of CS and perturbation

3.6 CS dynamics with random gradient of parameter

Till now we studied CS dynamics for periodic modulation of parameters and constant gradient. However, a practical system may have a random fluctuations or gradients of parameter to address that we study CS dynamics with random gradient of parameter. By taking $\mu = 1.37$ and $\gamma = 0.5$, the pump parameter for active and passive material

respectively and having random fluctuations, the following results were monitored. CS was formed in the form of the multiple numbers of branches which are unequally spaced and are of different amplitude.

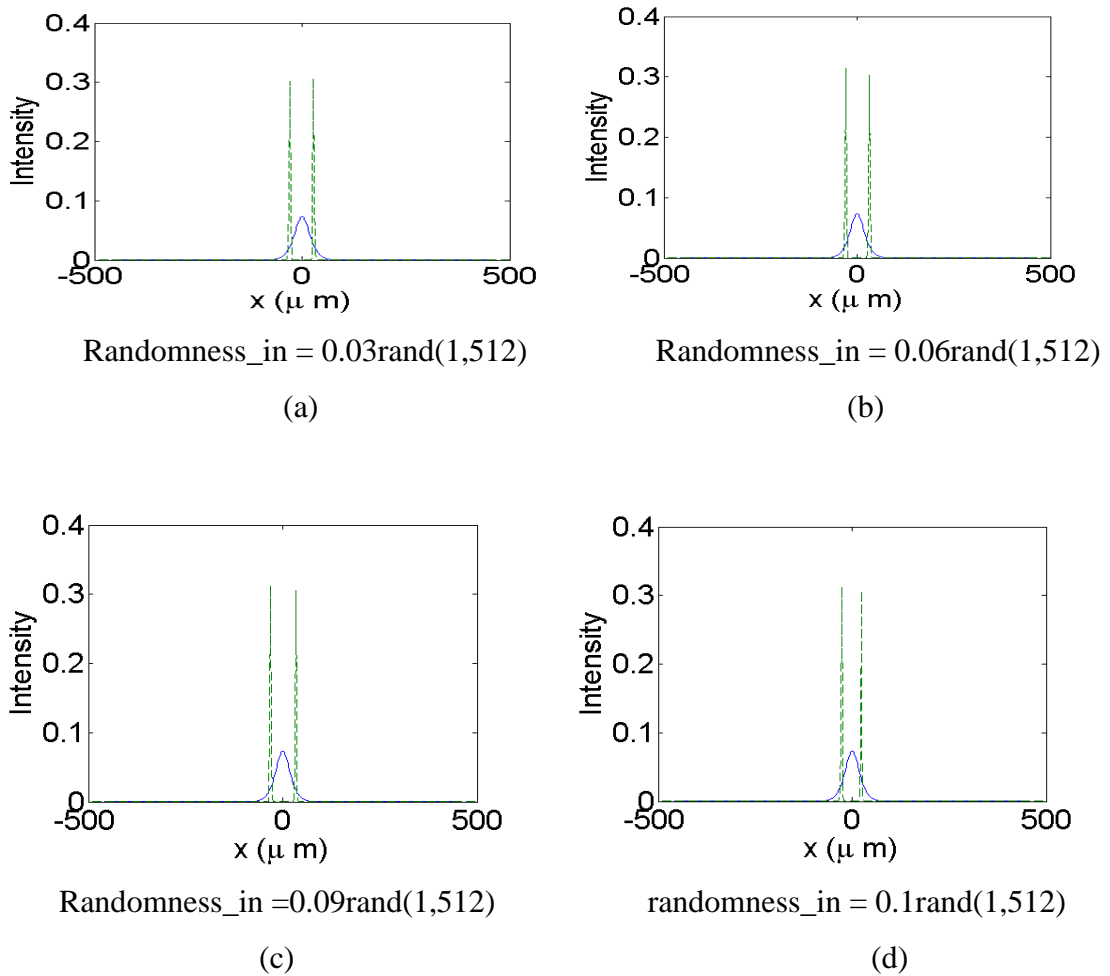


Figure 3.17 (a) to (d) the dynamics of CS with random parameter gradient

The branches move towards the zero point as modulation is applied. But at 0.09 and 0.4 perturbation branch move away from the zero point.

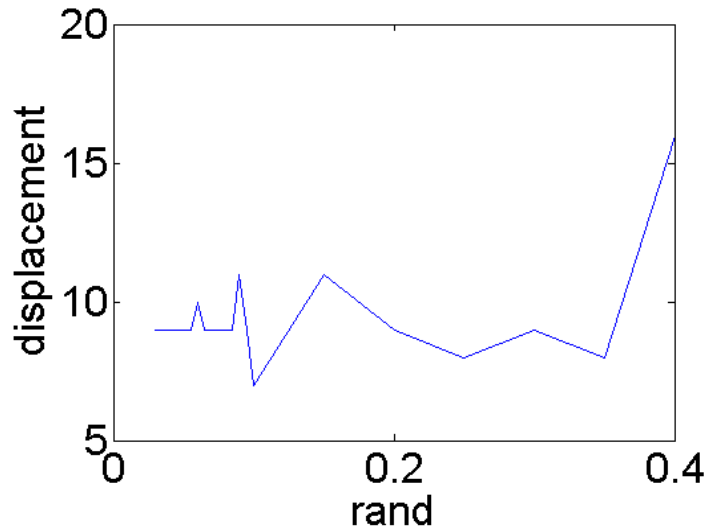


Figure 3.18 The plot between displacement of CS and randomness

Conclusion:-

Cavity soliton are generated in a VCSEL with a saturable absorber and is paired to an external FSF (frequency selective feedback) element. We studied the dynamics of cavity soliton for different periodic modulation of parameters and constant gradient of parameters. We also studied CS dynamics for random fluctuation or gradient of system parameter which is very practical situation. The effect of gradient or fluctuation in parameter has been extensively presented. This result of CS dynamics can be used to scan inhomogenities available in broad-area system. These results promise soliton force microscopy. However, several challenges like inadequate resolution and insufficient sensitivity need to be overcome before experimental realization.

List of figures

Figure 2.1(a) Fundamental Soliton, (b) second order soliton

Figure 2.2 Soliton collision

Figure 2.3 Conservative soliton

Figure 2.4 Dissipative soliton

Figure 2.5 Optical Cavity Soliton

Figure 2.6 Typical VCSEL

Figure 2.7 Structure of VCSEL

Figure 2.8 Edge emitting and VCSEL

Figure 2.9 Scanning Probe Microscopy

Figure 2.10 Scheme for CS generation in VCSEL coupled with frequency selective feedback

Figure 2.11 Schematic diagram of symmetrized split step fourier method

Figure 3.1 Variation of pump parameter μ for $\sin(r)$ gradient function

(a) $\mu=1.365+0.015\sin(r)$ (b) $\mu=1.365+0.02\sin(r)$

(c) plot of displacement of CS and modulation of parameter.

Figure 3.2 Variation of μ pump parameter for $\cos(r)$ gradient function

(a) $\mu=1.365+0.01\cos(r)$ (b) $\mu=1.365+0.025\cos(r)$

(c) $\mu=1.365+0.035\cos(r)$ and (d) plot of displacement of CS and perturbation

Figure 3.3(a) to (d) variation of μ pump parameter for linear gradient function $f(r)=r$ and (e) plot of modulation of gradient function and displacement

Figure 3.4(a)(b) variation of μ pump parameter for r^2 gradient function and (c) displacement of CS Vs perturbation plot

Figure 3.5 Variation of pump parameter γ for $\sin(r)$ gradient function

(a) $\gamma=0.5+0.01\sin(r)$ (b) $\gamma=0.5+0.04\sin(r)$

(c) $\gamma=0.5+0.08\sin(r)$ (d) $\gamma=0.5+0.1\sin(r)$

(e) plot between displacement of CS and perturbation

Figure 3.6 Variation of pump parameter γ for $\cos(r)$ gradient function

(a) $\gamma=0.5+0.01\cos(r)$ (b) $\gamma=0.5+0.04\cos(r)$

(c) $\gamma=0.5+0.08\cos(r)$ (d) $\gamma=0.5+0.1\cos(r)$

(e) plot between displacement of CS and perturbation

Figure 3.7 Variation of pump parameter γ for r linear gradient function

- (a) $\gamma = 0.5 + 0.00001r$ (b) $\gamma = 0.5 + 0.00003r$
 (c) $\gamma = 0.5 + 0.000045r$ (d) $\gamma = 0.5 + 0.00007r$
 (e) plot between displacement of CS and perturbation

Figure 3.8 (a) plot of displacement of CS and modulation of parameter.

- (b) $\gamma = 0.5 + 0.0000001r^2$ (c) $\gamma = 0.5 + 0.0000002r^2$
 (d) $\gamma = 0.5 + 0.00000035r^2$ (e) $\gamma = 0.5 + 0.0000008r^2$

Figure 3.9 Variation of μ pump parameter for $\sin(r)$ function

- (a) $\mu = 1.365 + 0.02 \sin(r)$ (b) $\mu = 1.365 + 0.03 \sin(r)$
 (c) perturbation and displacement of CS plot

Figure 3.10 Variation in μ pump parameter for $\cos(r)$ periodic gradient function

- (a) $\mu = 1.365 + 0.01 \cos(r)$ (b) $\mu = 1.365 + 0.02 \cos(r)$
 (c) $\mu = 1.365 + 0.025 \cos(r)$ (d) $\mu = 1.365 + 0.04 \cos(r)$
 (e) perturbation Vs displacement of CS plot

Figure 3.11 Variation of μ pump parameter for r linear gradient function

- (a) $\mu = 1.365 + 0.00015r$ (b) $\mu = 1.365 + 0.0002r$
 (c) perturbation Vs displacement of CS plot

Figure 3.12 Variation of μ pump parameter r^2 gradient function

- (a) $\mu = 1.365 + 0.0000001r^2$ (b) $\mu = 1.365 + 0.00000025r^2$
 (c) plot between displacement and perturbation

Figure 3.13 Variation of γ pump parameter for $\sin(r)$ gradient function

- (a) $\gamma = 0.5 + 0.02 \sin(r)$ (b) $\gamma = 0.5 + 0.045 \sin(r)$
 (c) $\gamma = 0.5 + 0.08 \sin(r)$ (d) $\gamma = 0.5 + 0.095 \sin(r)$
 (e) perturbation Vs displacement of CS plot

Figure 3.14 Variation of γ pump parameter for $\cos(r)$ gradient function

- (a) $\gamma = 0.5 + 0.02 \cos(r)$ (b) $\gamma = 0.5 + 0.05 \cos(r)$
 (c) $\gamma = 0.5 + 0.065 \cos(r)$ (d) $\gamma = 0.5 + 0.09 \cos(r)$
 (e) plot between perturbation and displacement of CS

Figure 3.15 Variation of γ pump parameter for r linear gradient function

- (a) $\gamma = 0.5 + 0.000015r$ (b) $\gamma = 0.5 + 0.00005r$
 (c) $\gamma = 0.5 + 0.00007r$ (d) $\gamma = 0.5 + 0.000085r$
 (e) plot between perturbation and displacement of CS

Figure 3.16 Variation of γ pump parameter using r^2 gradient function

- (a) $\gamma = 0.5 + 0.0000004r^2$ (b) $\gamma = 0.5 + 0.00000085r^2$
 (c) plot between displacement of CS and perturbation

Figure 3.17(a) to (d) the dynamics of CS with random parameter gradient

Figure 3.18 The plot between displacement of CS and randomness.

REFERENCES

1. www.funFACS.org
2. Akhmediev N, General Theory of solitons, Kluwer Academic Publishers, 2001:371-395.
3. Firth WJ, Paulau P V, Soliton lasers stabilized by coupling to a resonant linear system, *Eur Phys J D*, 2010;59(1):13–21.
4. Pedaci F, Tissoni G, Barland S, Giudici M, Tredicce J, Mapping local defects of extended media using localized structures, *Appl Phys Lett*. 2008;93(11).
5. Barbay S, Kuszelewicz R, Tredicce JR, Cavity solitons in VCSEL devices. *Adv Opt Technol*. 2011;2011.
6. B. KAUR, S. JANA, Generation and dynamics of one- and two-dimensional cavity solitons in a vertical-cavity surface-emitting laser with a saturable absorber and frequency-selective feedback, 2017;34(7):1374–85.
7. Akhmediev N, Soto-Crespo JM, Grapinet M, Grelu P, Dissipative soliton interactions inside a fiber laser cavity, *Opt Fiber Technol*, 2005;11(3):209–28.
8. J. Soumendu, Konar swapan, Non linear pulse and beam propagation, 2007:1-30
9. Rotschild C, Alfassi B, Cohen O, Segev M, Long-range interactions between optical solitons, *Nat Phys [Internet]*, 2006;2(11):769–74.
10. Ackemann T, Firth WJ, Oppo GL, Chapter 6 Fundamentals and Applications of Spatial Dissipative Solitons in Photonic Devices, *Adv At Mol Opt Phys*. 2009;57(March 2009):323–421.
11. McIntyre C, Dynamics and Interactions of Cavity Solitons in Photonic Devices, 2013
12. Akhmediev N, Dissipative Soliton, 2000, 1-417 p.
13. Yin C, Mihalache D, He Y, Dynamics of two-dimensional dissipative spatial solitons interacting with an umbrella-shaped potential, *J Opt Soc Am B [Internet]*, 2011;28(2):342.
14. Edwin D, Stability analysis of cavity solitons governed by the cubic-quintic Ginzburg–Landau equation, *Journal of Physics B*, 2011
15. Eslami M, Kheradmand R, Hashemvand G, The effect of nonlinear gain on the characteristics of an optically injected VCSEL and cavity solitons, *Opt Quantum Electron*. 2014;46(2):319–29.

16. Tissoni G, Aghdami KM, Prati F, Brambilla M, Lugiato LA, Cavity soliton laser based on a VCSEL with saturable absorber, *Localized States Phys Solitons Patterns*, 2011;920:187–211.
17. Panajotov K, Tlidi M, Spontaneous motion of cavity solitons in vertical-cavity lasers subject to optical injection and to delayed feedback, *Eur Phys J D*. 2010;59(1):67–72.
18. Prati F, Aghdami KM, Tissoni G, Brambilla M, Lugiato LA, Moving cavity solitons in a cavity soliton laser. *CLEO/Europe - EQEC 2009 - Eur Conf Lasers Electro-Optics Eur Quantum Electron Conf*, 2009;193(2003):4244.
19. Grelu P, Chouli S, Soto-Crespo JM, Chang W, Ankiewicz A, Akhmediev N, Dissipative solitons for mode-locked fiber lasers, *2010 Photonics Glob Conf PGC 2010*. 2010;6.
20. Tanguy Y, Ackemann T, Firth WJ, Jger R, Realization of a semiconductor-based cavity soliton laser, *Phys Rev Lett*. 2008;100(1):1–4.
21. Genevet P, Barland S, Giudici M, Tredicce JR, Cavity soliton laser based on mutually coupled semiconductor microresonators, *Phys Rev Lett*. 2008;101(12):1–4.
22. Tlidi M, Vladimirov AG, Pieroux D, Turaev D, Spontaneous motion of cavity solitons induced by a delayed feedback, *Phys Rev Lett*. 2009;103(10):1–4.
23. Scroggie AJ, Firth WJ, Oppo GL, Cavity-soliton laser with frequency-selective feedback, *Phys Rev A*. 2009;80(1):1–9.
24. Brambilla M, Lugiato LA, Prati F, Spinelli L, Firth WJ, Spatial Soliton Pixels in Semiconductor Devices, *Phys Rev Lett* .1997:2042-2045.
25. Munteanu L, Donescu S, Introduction to soliton theory: applications to mechanics, 2004. 308.
26. Kharenko DS, Babin SA, Generation of dissipative solitons in femtosecond fiber lasers, *Optoelectron Instrum Data Process*, 2013:399-415
27. Wise FW, Femtosecond fiber lasers based on dissipative processes for nonlinear microscopy, *IEEE J Sel Top Quantum Electron*. 2012;18(4):1412–21.
28. Prati F, Lugiato LA, Tissoni G, Brambilla M. Cavity soliton billiards. *Phys Rev A - At Mol Opt Phys*. 2011;84(5):1–6.
29. Iga K, Surface-emitting laser - its birth and generation of new optoelectronics field. *IEEE J Sel Top Quantum Electron*, 2000;6(6):1201–15.
30. Michalzik R. VCSELs, 2013;166:3–19.

31. Eslami M, Kheradmand R, Aghdami KM, Complex behavior of vertical cavity surface emitting lasers with optical injection. *Phys Scr* [Internet]. 2013;T157(T157):14038.
32. Volakis JL, Science C, Arbor A, low-threshold electrically pumped high-frequency performance of npn AlGaAs / GaAs heterojunction bipolar transistors. 1989;(17):1123–4.
33. Tlidi M, Panajotov K, Staliunas K, Phase-bistable patterns and cavity solitons induced by spatially periodic injection into vertical-cavity surface-emitting lasers. *Phys Rev A - At Mol Opt Phys*. 2014;89(5):1–5.
34. Agrawal G, *Nonlinear Fiber Optics*, Academic Press, San Diego, 2007;552.
35. Fibres O, Fourier S. *Numerical Tools for Simulation of Pulse Propagation in Optical Fibres*.